Some issues at the interface of strongly nonlinear space and fusion plasma physics

Richard Dendy

Euratom/UKAEA Fusion Association
Culham Science Centre
Abingdon, Oxfordshire OX14 3DB, U.K.

Centre for Fusion, Space and Astrophysics
Department of Physics, Warwick University
Coventry CV4 7AL, U.K.

Work supported in part by UK Engineering and Physical Sciences Research Council

Dennis Papadopoulos: his part in my downfall

- "Papadopoulos, Goldstein and Smith (*Astrophys. J.* **190**, 175 (1974)) have examined wave-trapping in cavitons as a mechanism for rapidly shifting electrostatic waves out of resonance with an electron beam in the context of Type III solar radio bursts"
  – R O Dendy, D Phil Thesis, p.5, Oxford University (1983)

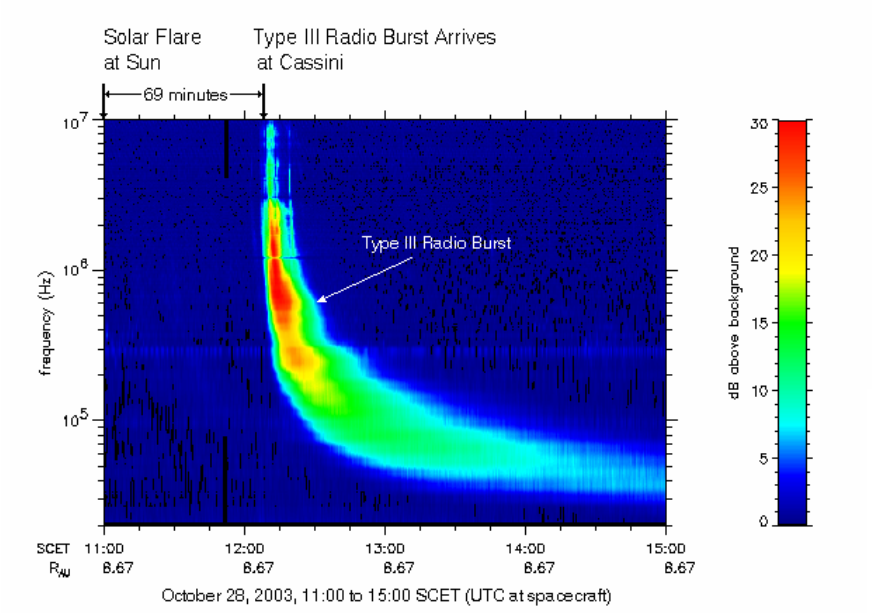

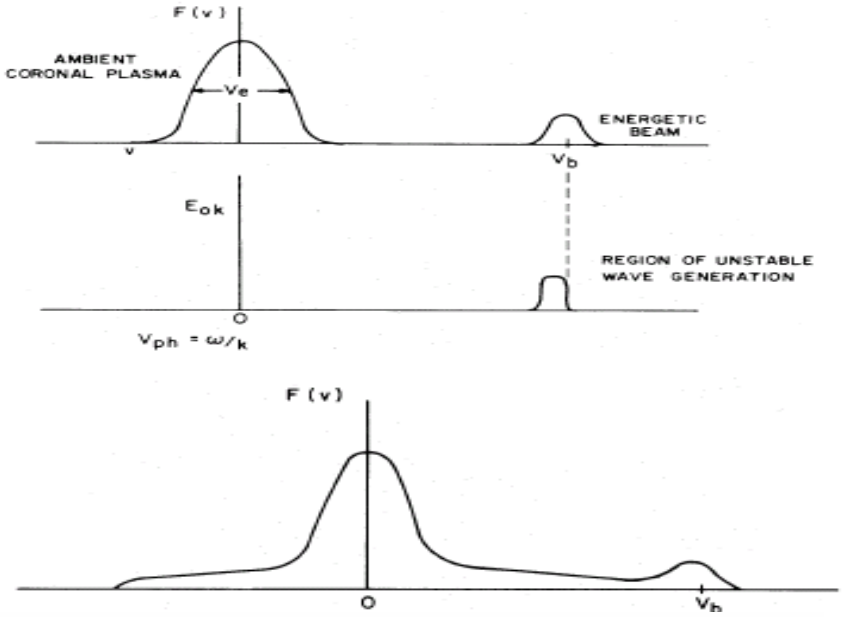

Let us examine now the nonlinear effects introduced by the oscillating two-stream instability. As the unstable waves grow in the region resonant with the beam, the background plasma sees at time t a field oscillating with frequency $\omega_0 \sim \omega_e$ and amplitude $E_0(t)$. When this field exceeds the threshold field given by equation (8), the oscillating two-stream instability starts pumping wave energy out of the mode k, into plasma oscillations with lower phase velocity (fig. 3) and zero-frequency (i.e., purely growing) ion density fluctuations. This effect removes plasma waves from resonance with the beam, and may cut off formation of the plateau if the growth time of the new waves becomes shorter than the generation time of the resonant waves.

CFSA centre for fusion, space and astrophysics

UKAEA Fusion Working in Europe

Strongly nonlinear signals from solar and astrophysical plasmas: key examples

Full disk solar EUV/XUV Emission

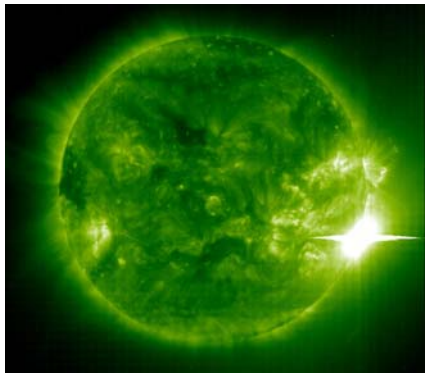

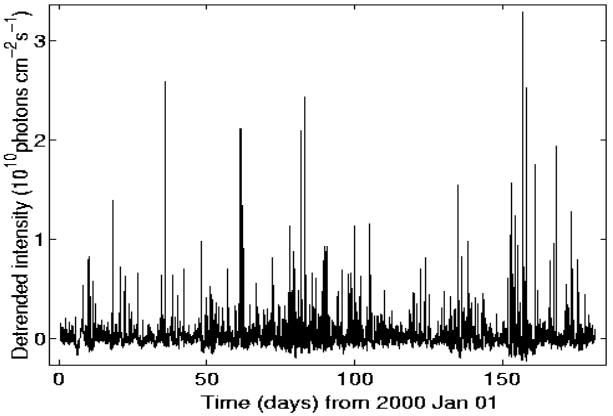

X-ray binary Cygnus X-1

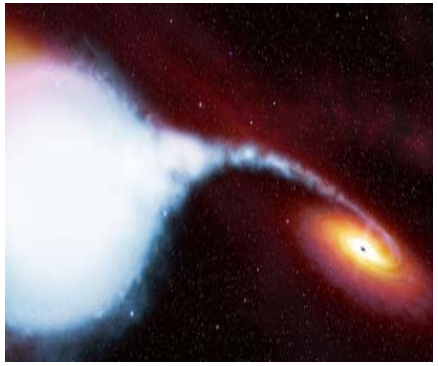

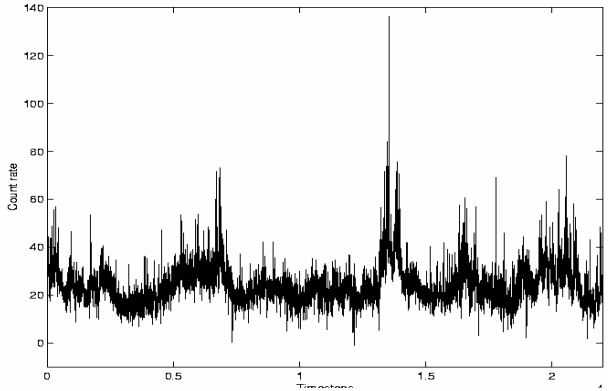

Microquasar GRS 1915

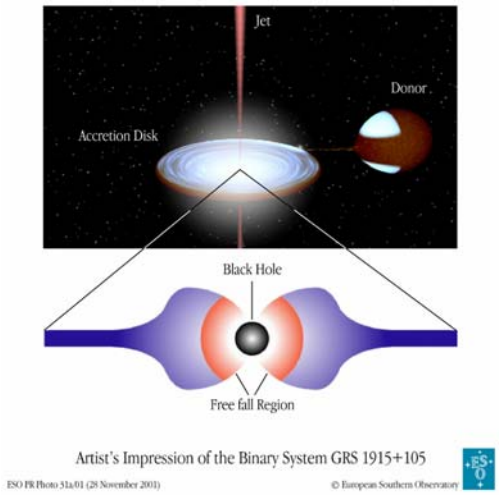

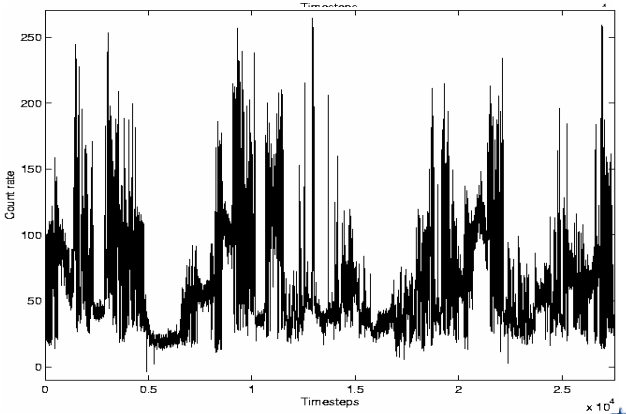

Strongly nonlinear signals from fusion plasmas: key examples

Edge turbulence in the Mega Amp Spherical Tokamak (MAST)

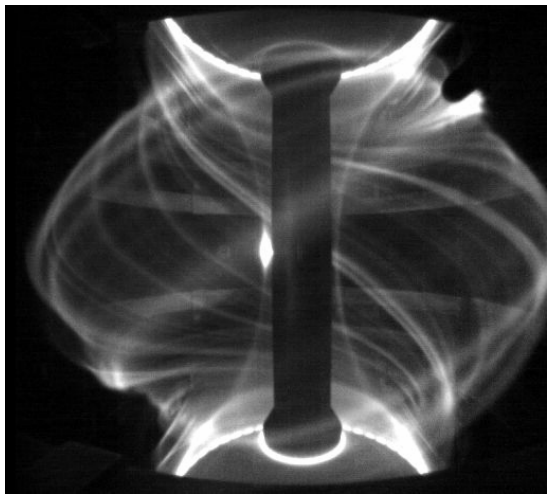

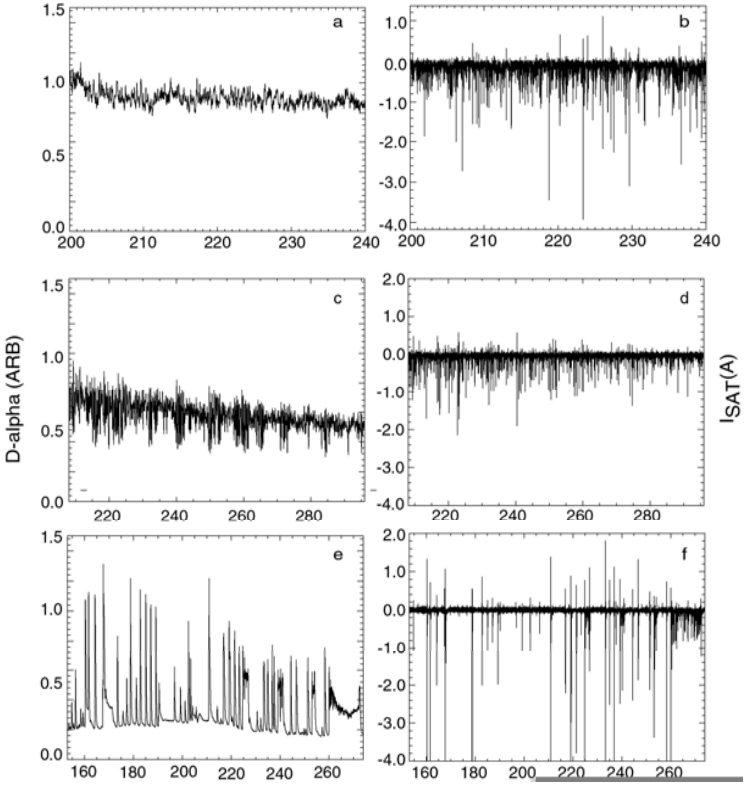

Edge localised modes in the Joint European Torus (JET)

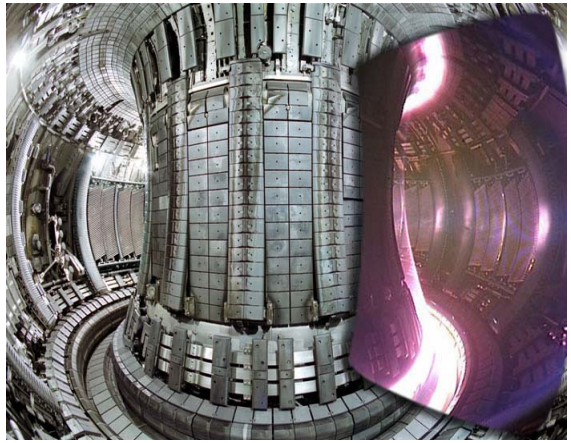

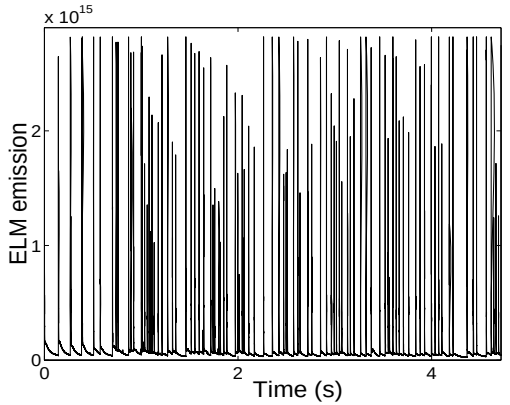

CFSA centre for fusion, space and astrophysics

UKAEA Fusion Working in Europe

Probability density function of X-ray time series: Cygnus X-1

- Not classical:
  - Gaussian (black dash)
  - Log-normal (green dots)
- Extreme event distributions:
  - Small amplitude Gumbel (blue dash a = 1, blue solid a = 2)
  - Large amplitude Fréchet (red solid a = 1.1)

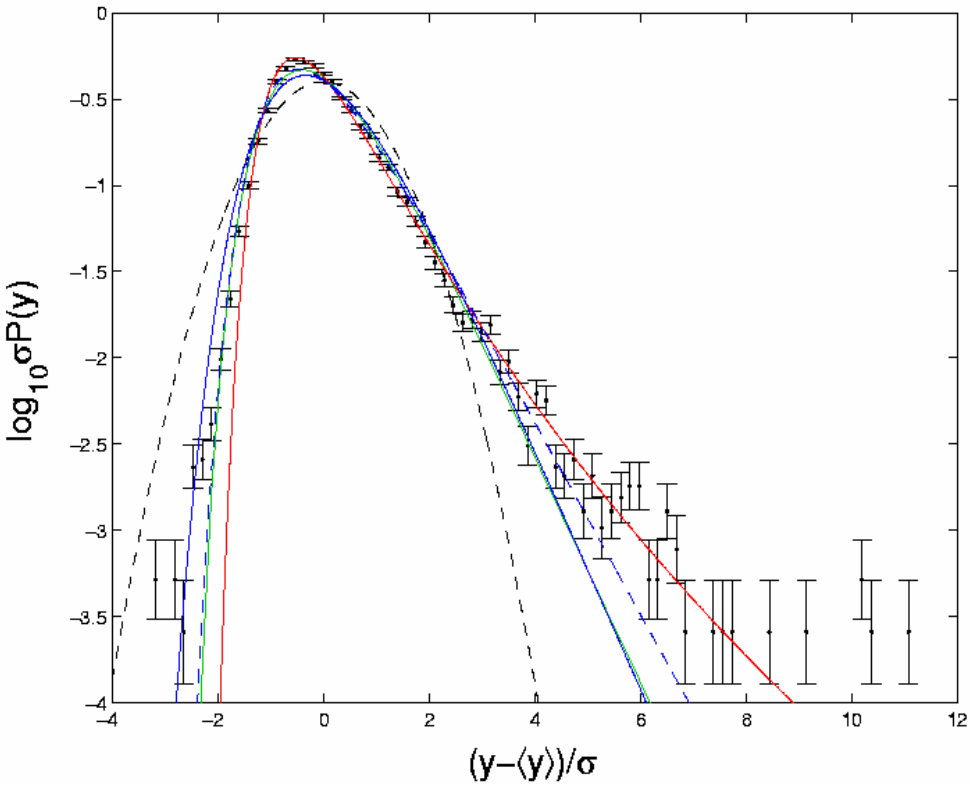

Greenhough *et al., Astron. Astrophys.* **385**, 693 (2002)

CFSA centre for fusion, space and astrophysics

UKAEA Fusion Working in Europe

Probability density function: GRS 1915+105

- Not classical:
  - Gaussian (black dash)
  - log-normal (green dots)
- Extreme event distributions:
  - Small amplitude Fréchet (red solid a = 1.1)
  - Large amplitude Gumbel (blue dash a = 1, blue solid a = 2)
- Several peaks

  ⇒ multi-component source

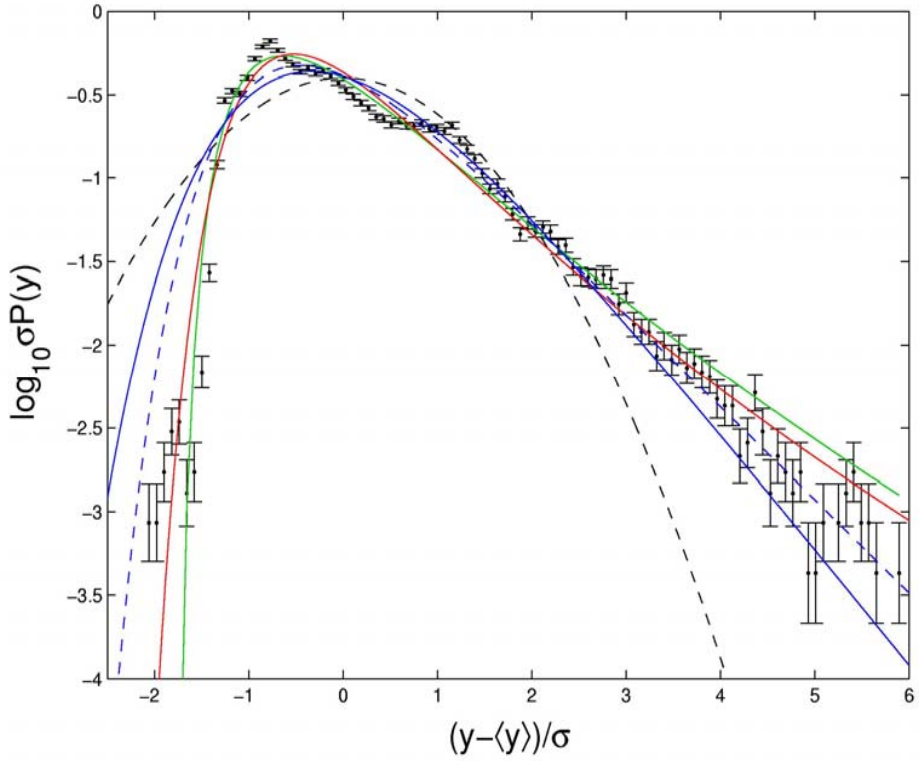

Extreme value PDFs of I_{SAT} for three MAST Ohmic L-mode plasmas

Measured frequency of occurrence of ion saturation current amplitude, sampled at 500kHz and summed over timescale $\tau = 2\mu s$ (left) and $64\mu s$ (right). Red curves: extreme value distributions fitted.

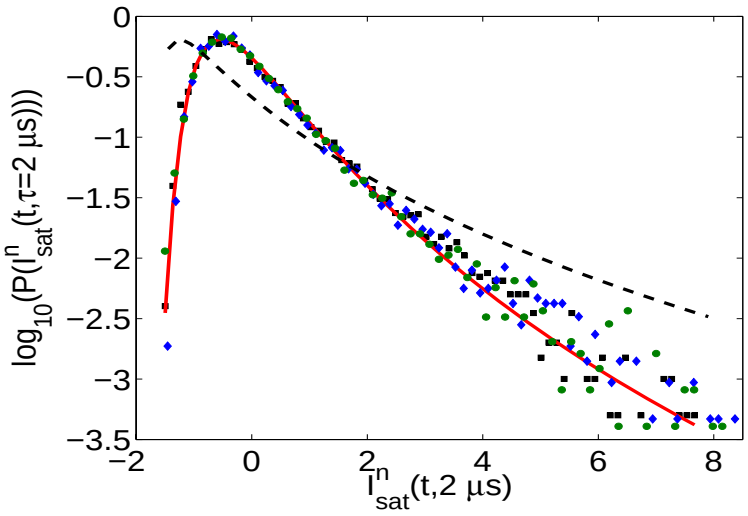

Fréchet $k = 1.0$

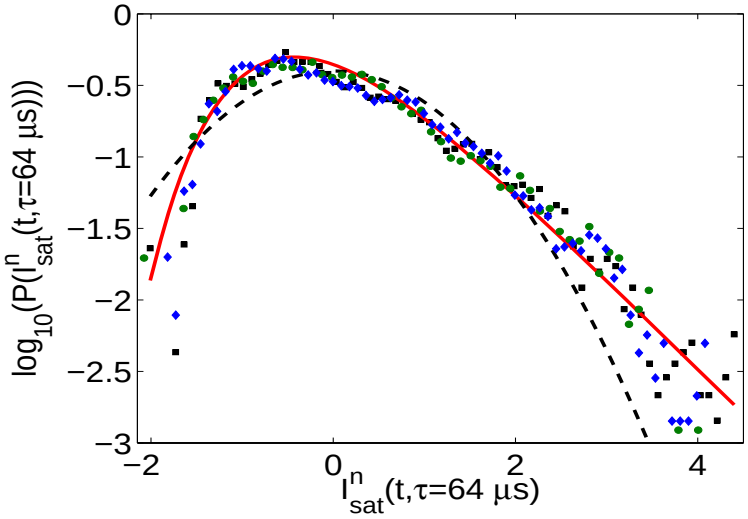

Gumbel $a = 1.4$

Dashed lines: log-normal (left) and normal (right) with same μ and σ as data.

Hnat, Dudson, Dendy *et al., Nuclear Fusion* **48**, 085009 (2008)

CFSA centre for fusion, space and astrophysics

UKAEA Fusion Working in Europe

Triangulating fusion plasma turbulence

There is a quest to understand the extent (if any) of "universality" – i.e. shared, scalable phenomenology – in plasma turbulence in the three main toroidal magnetic confinement approaches:

Large aspect ratio tokamak:

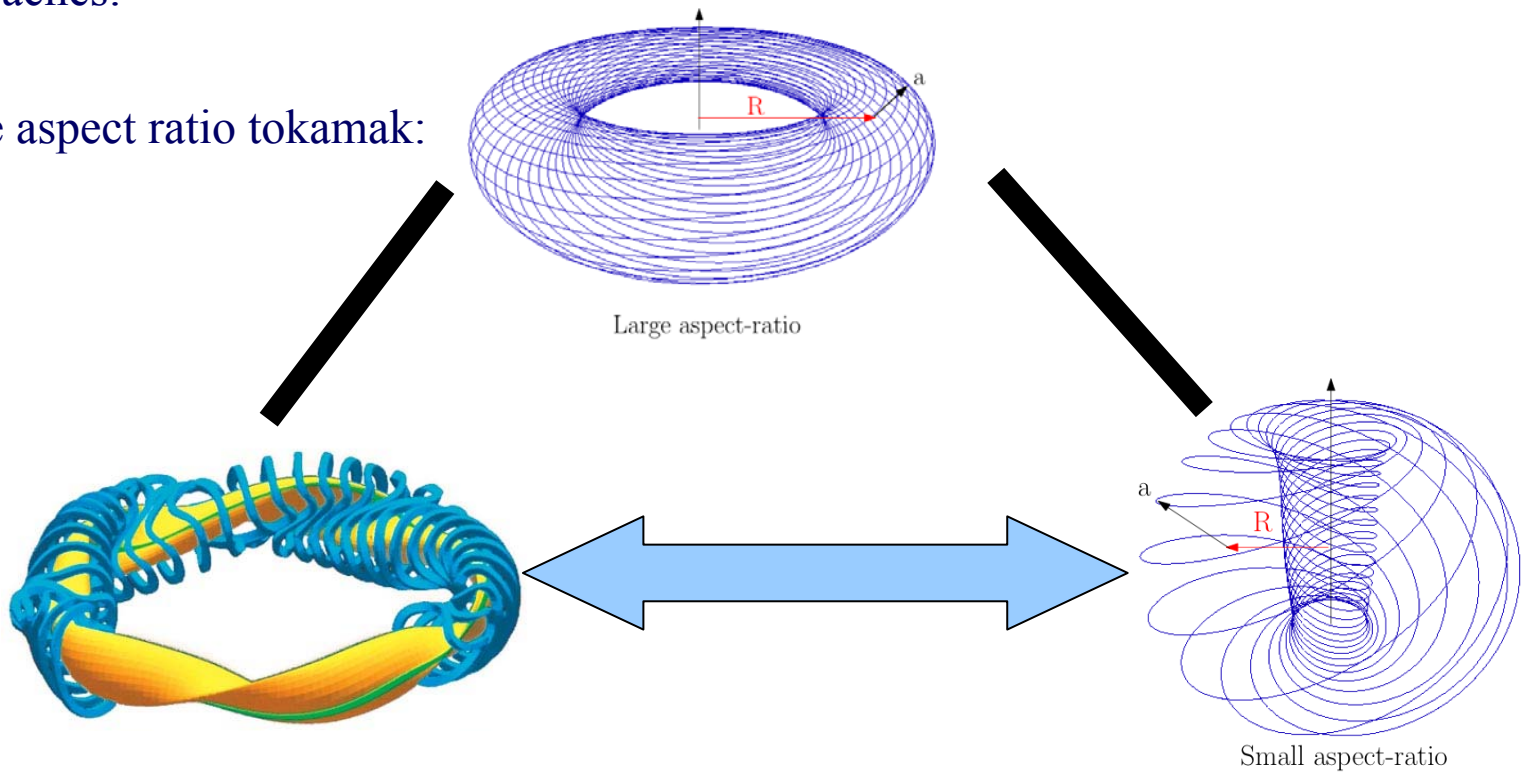

Stellarator

Spherical tokamak

CFSA centre for fusion, space and astrophysics

UKAEA Fusion Working in Europe

Comparing plasma turbulence in stellarator and spherical tokamak

The Mega Amp Spherical Tokamak, MAST, Euratom/UKAEA Culham

The Large Helical Device, LHD at NIFS, Tajimi, Japan

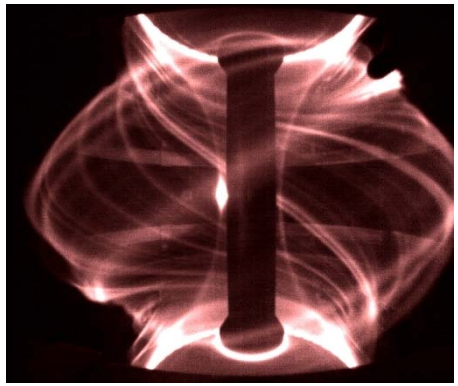

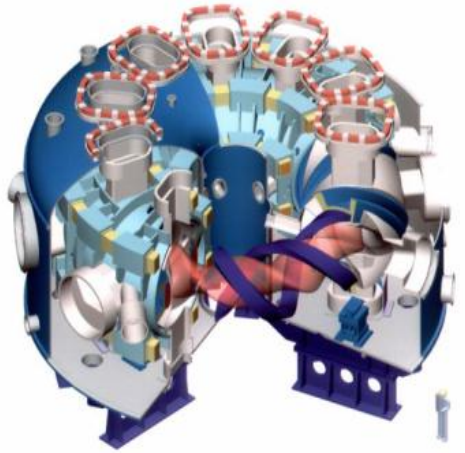

	Mega-Amp Spherical Tokamak (MAST)	Large Heical Device (LHD)
Device type	Spherical tokamak	Heliotron-type stellarator
Major radius, *R*	0.85m	3.9m
Minor radius, *a*	0.65m	0.65m
Typical magnetic field strength	0.5T	2.5T
Probe type	Reciprocating probe	3 pins separated by 6mm in a probe array
Probe location	Outboard midplane	Divertor plate
Sampling frequency	500kHz	250kHz
Typical length of time series	50ms / 25,000 samples	1s / 250,000 samples
Shot numbers	14218, 14219, 14220, 14222, 14260, 14264	44190, 44191

CFSA centre for fusion, space and astrophysics

UKAEA Fusion Working in Europe

Edge turbulence measurements from MAST and LHD

MAST

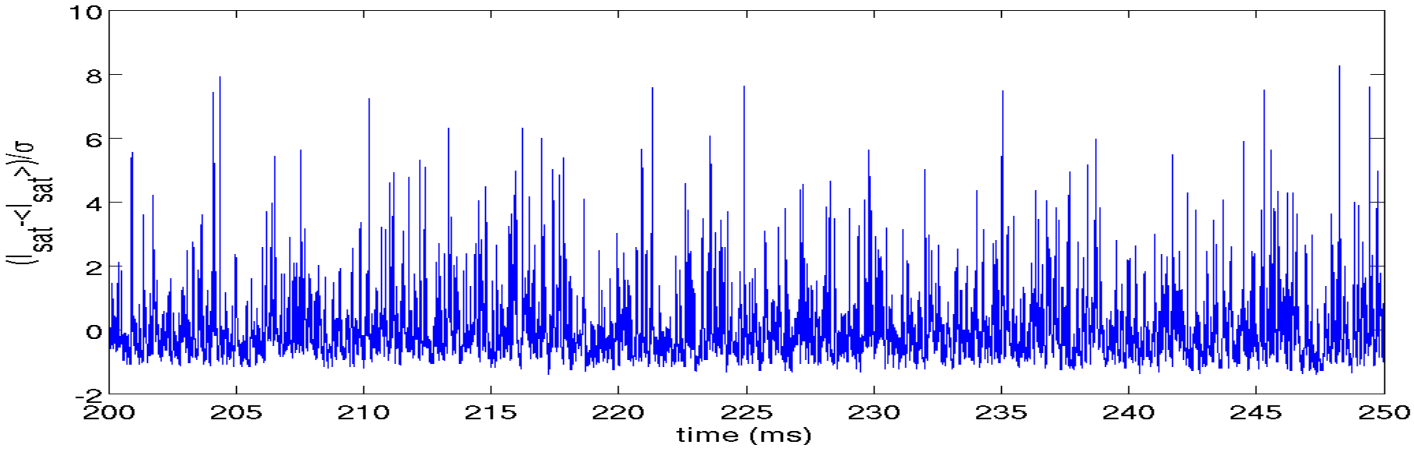

LHD

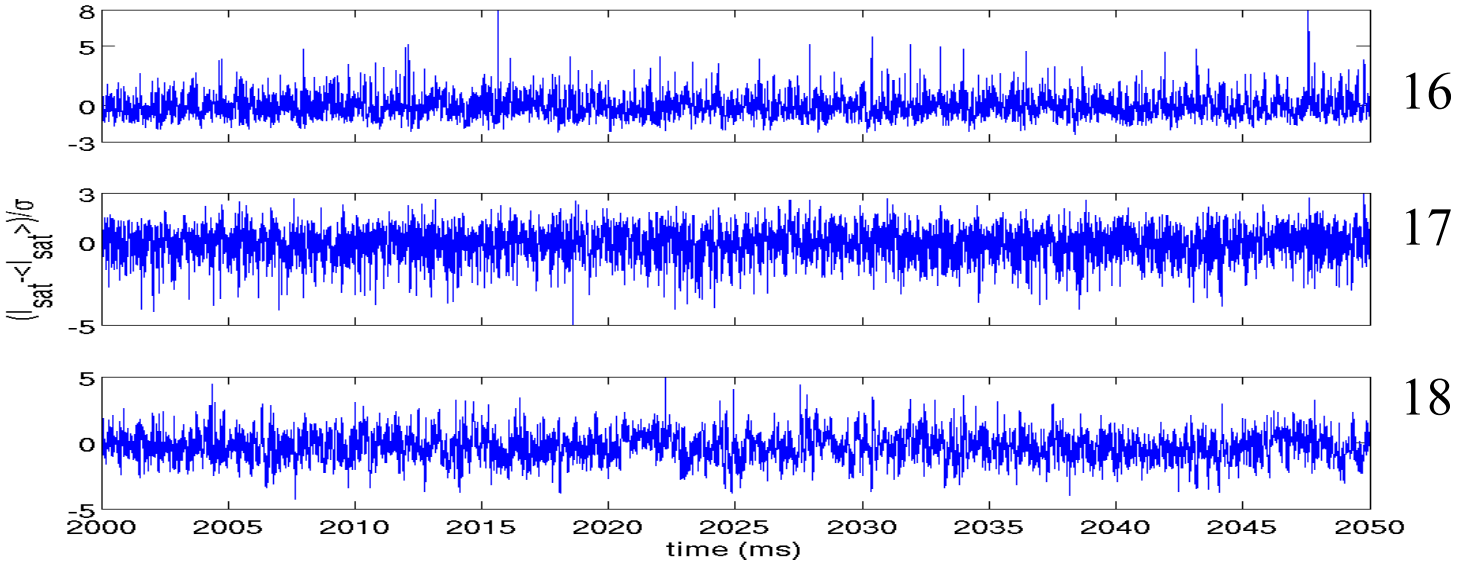

CFSA centre for fusion, space and astrophysics

UKAEA Fusion Working in Europe

Treatment of plasma turbulent fluctuation measurements

The inserted probes measure ion saturation current $I_{sat} \sim n_e T_e^{1/2}$. We know that we are addressing non-Maxwellian fluctuations with measured statistics:

MAST LHD (16) LHD (17) LHD (18)

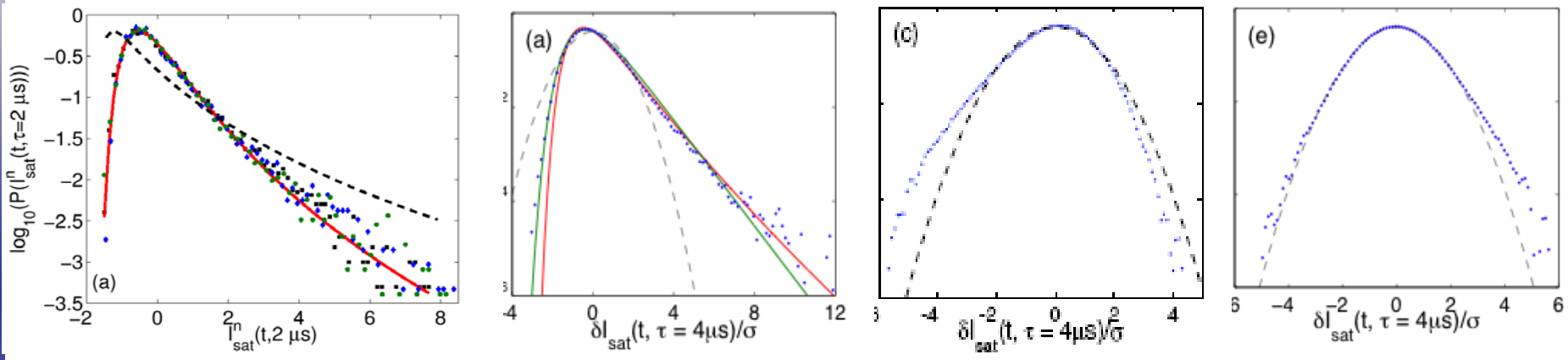

Treat each I_{sat} measurement as a stochastic increment, i.e. a step on a random walk, on the shortest possible timescale τ_{min} which is defined by the probe sampling rate. Fluctuations on longer timescales τ are constructed by summing and detrending:

$$\delta I_{sat}(t,\tau) = \sum_{t'=t}^{t+\tau-\tau_{min}} (I_{sat}(t') - \langle I_{sat}\rangle_t)/\sigma$$

The associated structure functions are constructed from the absolute moments

$$S_m(\tau) \equiv \langle |\delta x(t,\tau)|^m \rangle \propto \tau^{\xi(m)}$$

CFSA centre for fusion, space and astrophysics

UKAEA Fusion Working in Europe

Capturing statistical self similarity through structure functions

The generalised structure function $S(p, l)$ of order p on scale l, for a signal $z(x)$, is:

$$S(p, l) = < \{z(x + l) - z(x)\}^p >$$

Here $< >$ denotes an ensemble average – for example, an integral over x.

Simple self similarity is reflected empirically by *scaling* of the form

$$S(p, l) \sim l^{\zeta(p)}$$

Basic fluid turbulence models yield scaling that is linear in p, i.e. $\zeta(p) = ap$, so that

$$S(p, l) \sim l^{ap}$$

where the value of a may be inferred from theory, e.g.

$a = 1/3$ in Kolmogorov's fluid turbulence approach of 1941

$a = 1/4$ in the Iroshnikov-Kraichnan theory of Alfvénic MHD turbulence

In general, $\zeta(p)$, which arises from the cascade processes that constitute the turbulence:

-can be a nonlinear function of p, to capture intermittency, and

-may include terms reflecting dissipation.

Generalised structure functions for MAST and LHD turbulence

If we plot the logarithm of $S(p, l) = < \{z(x + l) – z(x)\}^p >$ against l for different p, basic turbulent scaling dependence of the form $S(p, l) \sim l^{ap}$ shows as linear traces.

Both MAST and LHD yield good scaling of this form, with two well defined scaling regions:

MAST[a] LHD[b]

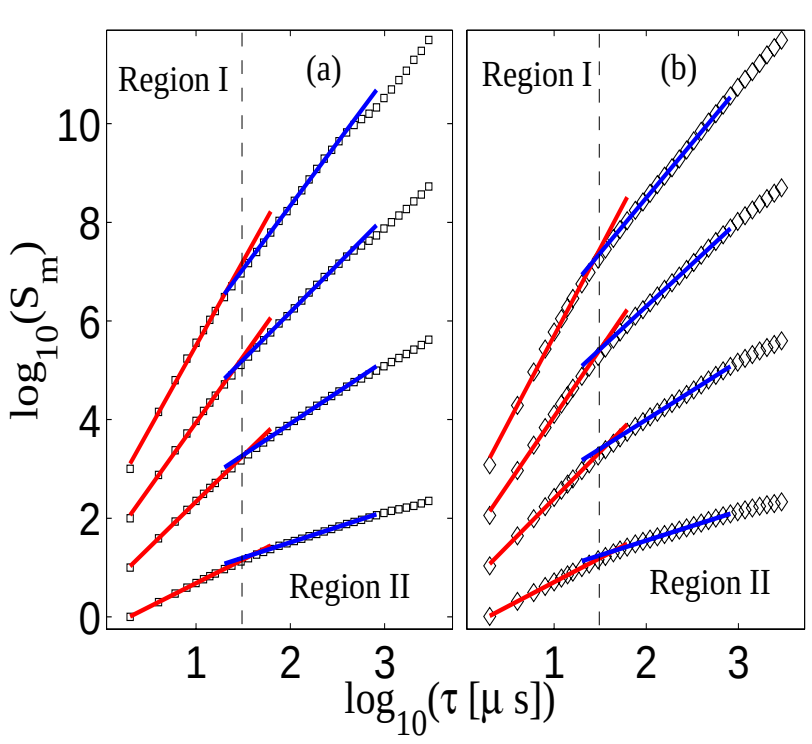

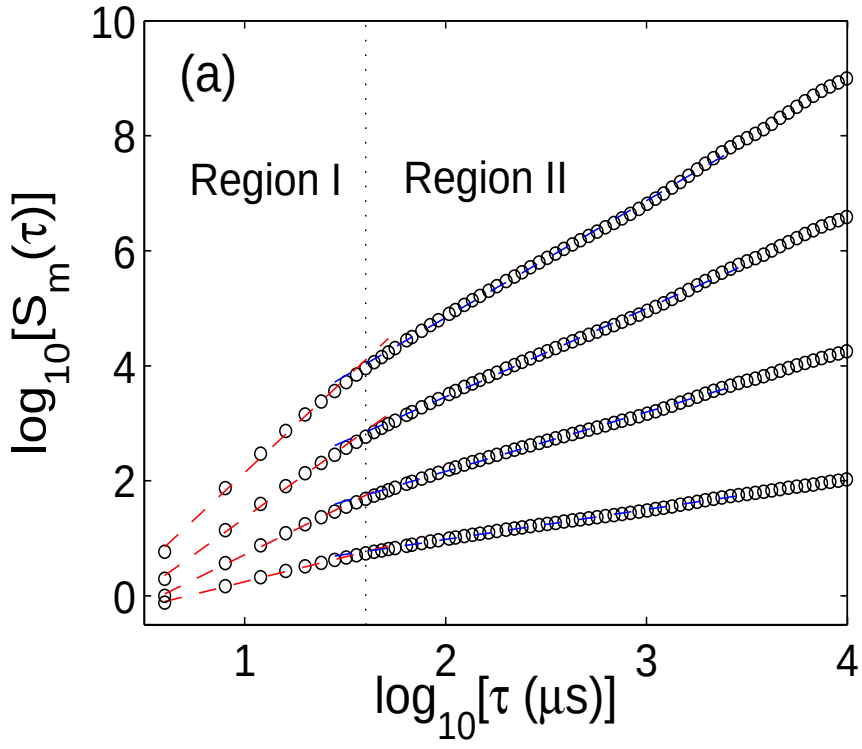

[a]Hnat *et al, Nucl Fusion* **48**, 85009 (2008)

[b]Dewhurst *et al, Plasma Phys Contr Fus* **50**, 95013 (2008)

CFSA centre for fusion, space and astrophysics

UKAEA Fusion Working in Europe

Scaling properties of turbulence in MAST and LHD

We have thus identified a regime corresponding to fluid turbulence having $S(p, l) \sim l^{ap}$, or equivalently for I_{sat} probe measurements

$$S_m(\tau) \equiv \langle |\delta x(t,\tau)|^m \rangle \propto \tau^{\zeta(m)}$$

with $\zeta(m) = \alpha m$ where α can be measured from the plots:

MAST

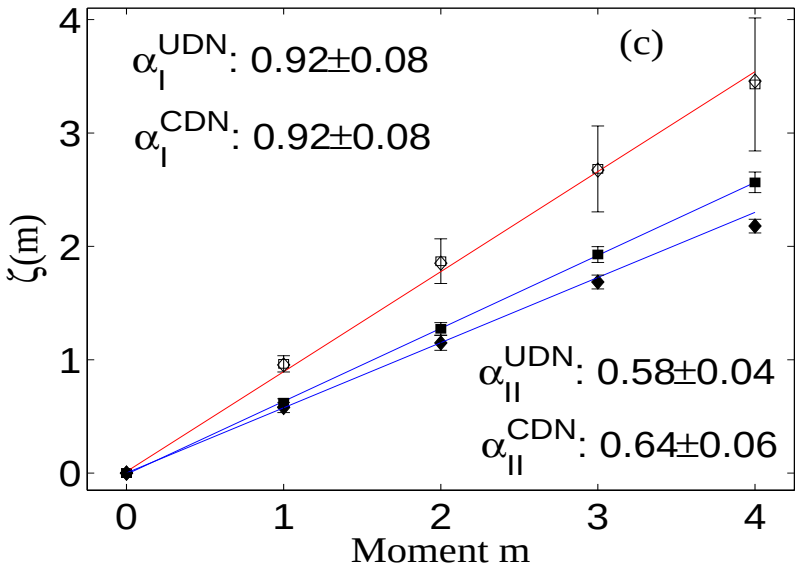

LHD

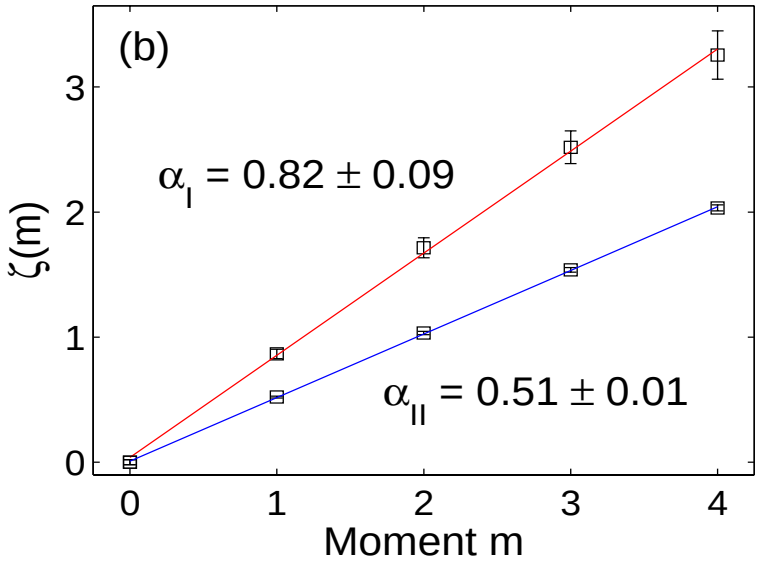

This provides rigorous quantification of plasma turbulence properties for comparison

-between different confinement systems

-between measurement and numerical simulations

CFSA centre for fusion, space and astrophysics

UKAEA Fusion Working in Europe

Structure function scaling beyond the ideal

Related question: what is "a turbulence theory"?

Even for linear fluid scaling, different cascade processes may operate over different ranges of separations l, hence

$$S(p, l) = < \{z(x + l) - z(x)\}^p > \sim l^{ap} \text{ for } l < L_1,$$
$$S(p, l) \sim l^{bp} \text{ for } l > L_1$$

Finite system size L_{max} affects large-l properties of $S(p, l)$

Dissipation on small scales affects small-l properties of $S(p, l)$

Real turbulent signals also typically reflect intermittency: meaning large events which, although infrequent, are so large that they cannot be "neglected" or "ordered out" – often a consequence of the rise and fall of the most strongly dissipating structures. Self similarity is then reflected empirically by scaling of the form

$$S(p, l) \sim l^{\zeta(p)}$$

where $\zeta(p)$ depends nonlinearly on p.

A model that predicts the functional form of $\zeta(p)$ from first principles, e.g. by linking it to the dimension of dissipating structures, is a turbulence theory.

Early example of application of extended self similarity

In 2000, Biskamp and Müller published a 512 cube simulation of MHD turbulence:

$k^{5/3}\,E(k)$ versus k

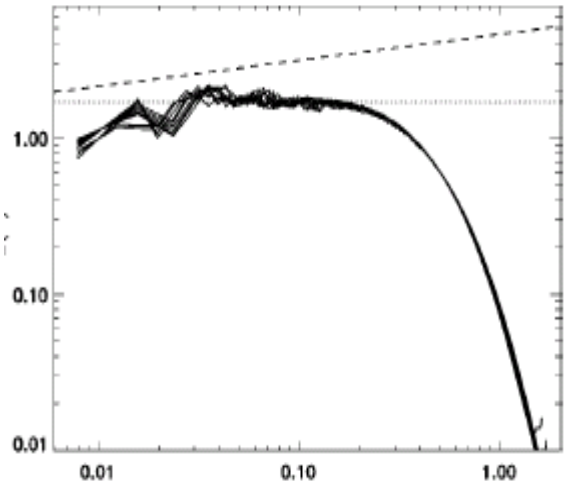

$\zeta(p)$ versus p

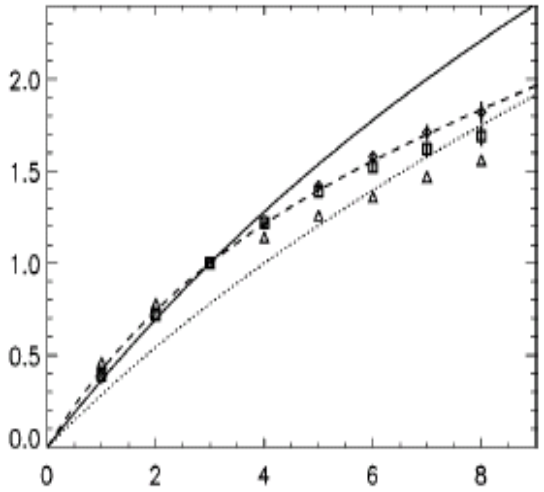

$S(5)$ versus $S(3)$

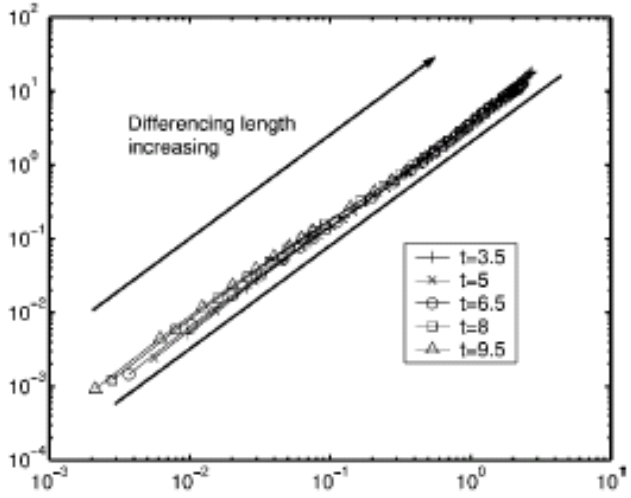

Addressing dissipative effects: extended self similarity

Given a plot of log $S(p, l)$ versus log l which is curved because of the consequences of dissipation, finite system size, intermittency, etc.,

Can the invariant statistical properties of a single underlying turbulent process, if one operates, nevertheless shine through?

Benzi *et al*. (Phys. Rev. E **48**, R29 1993) hypothesise that:

1. There is an unknown "generalised lengthscale" $G(l)$ instead of l, such that
   $S(p, l) \sim [G(l)]^{\zeta(p)}$ instead of $S(p, l) \sim l^{\zeta(p)}$
2. This generalised scaling penetrates into the dissipation range.

Hence formally $S(q, l) \sim [G(l)]^{\zeta(q)}$, and taking ratios of structure functions at two different orders, p and q

$$S(p, l) \sim [S(q, l)]^{\zeta(p)/\zeta(q)}$$

If, empirically, a plot of log $S(p + 2, l)$ versus log $S(p, l)$ yields a straight line, its gradient is $\zeta(p + 2)/\zeta(p)$, and this reflects extended self similarity ("ESS").

If the plot remains curved, this reflects deep nonlinear dependence of $\zeta(p)$ on p, due e.g. to intermittency

Solar wind plasma: a classic turbulence laboratory

-High magnetic Reynolds number, i.e. ratio of convective to dissipative terms

-Wide range of length scales, hence a well defined inertial range turbulent cascade

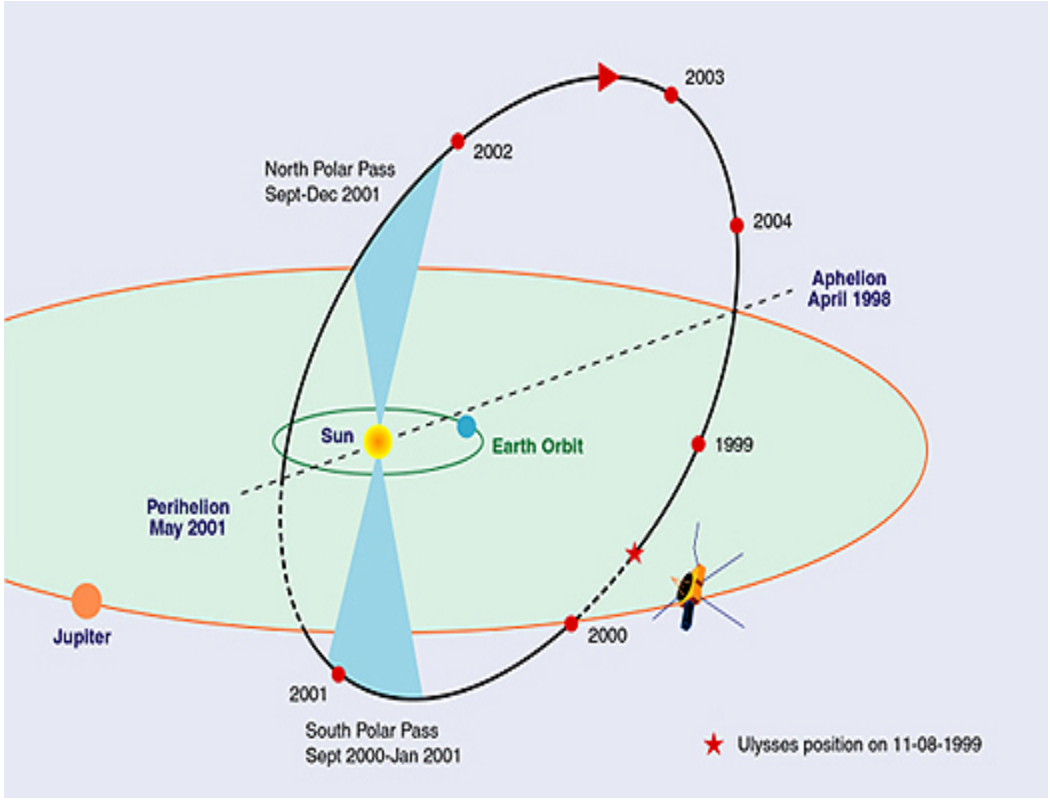

The Ulysses spacecraft has a unique out-of-ecliptic heliocentric orbit, achieved by gravity assistance from a Jupiter swing-by

Ulysses has spent many months above the sun's polar coronal holes, taking measurements of magnetic field components in the quiet fast solar wind

CFSA centre for fusion, space and astrophysics

UKAEA Fusion Working in Europe

Solar wind magnetic field power spectrum measured by Ulysses

Logarithmic plots of spectral power [nT^2/Hz] versus frequency [Hz] for the components of **B**

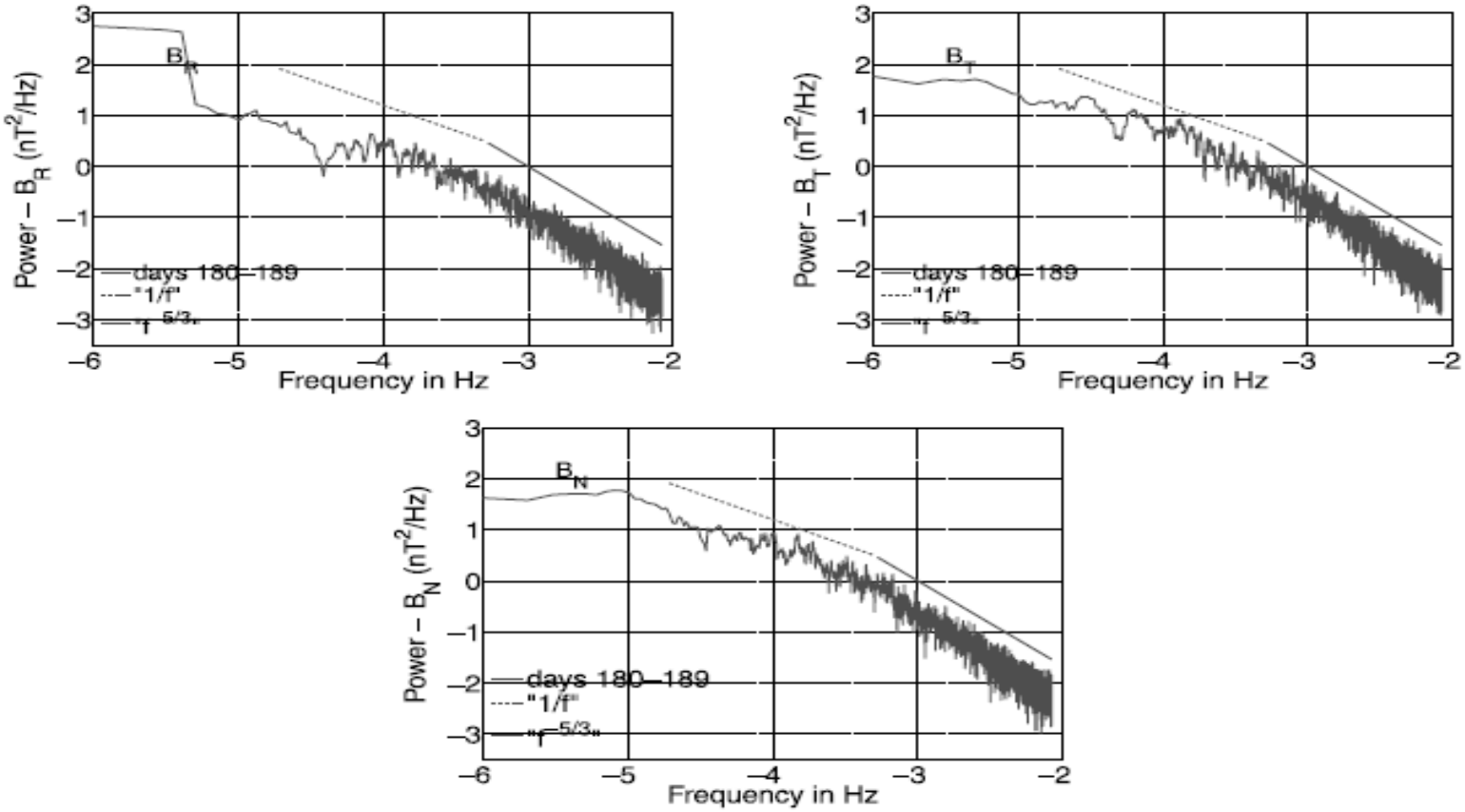

The low frequency $1/f$ range is probably due to the coronal driver of the solar wind

The high frequency $1/f^{5/3}$ inertial range is fairly well defined

CFSA centre for fusion, space and astrophysics

UKAEA Fusion Working in Europe

Scaling properties of the solar wind

Logarithmic plots of $S(p = 3, \tau)$ versus τ (Nicol *et al.*, *Astrophys J* 679, 862 (2008))

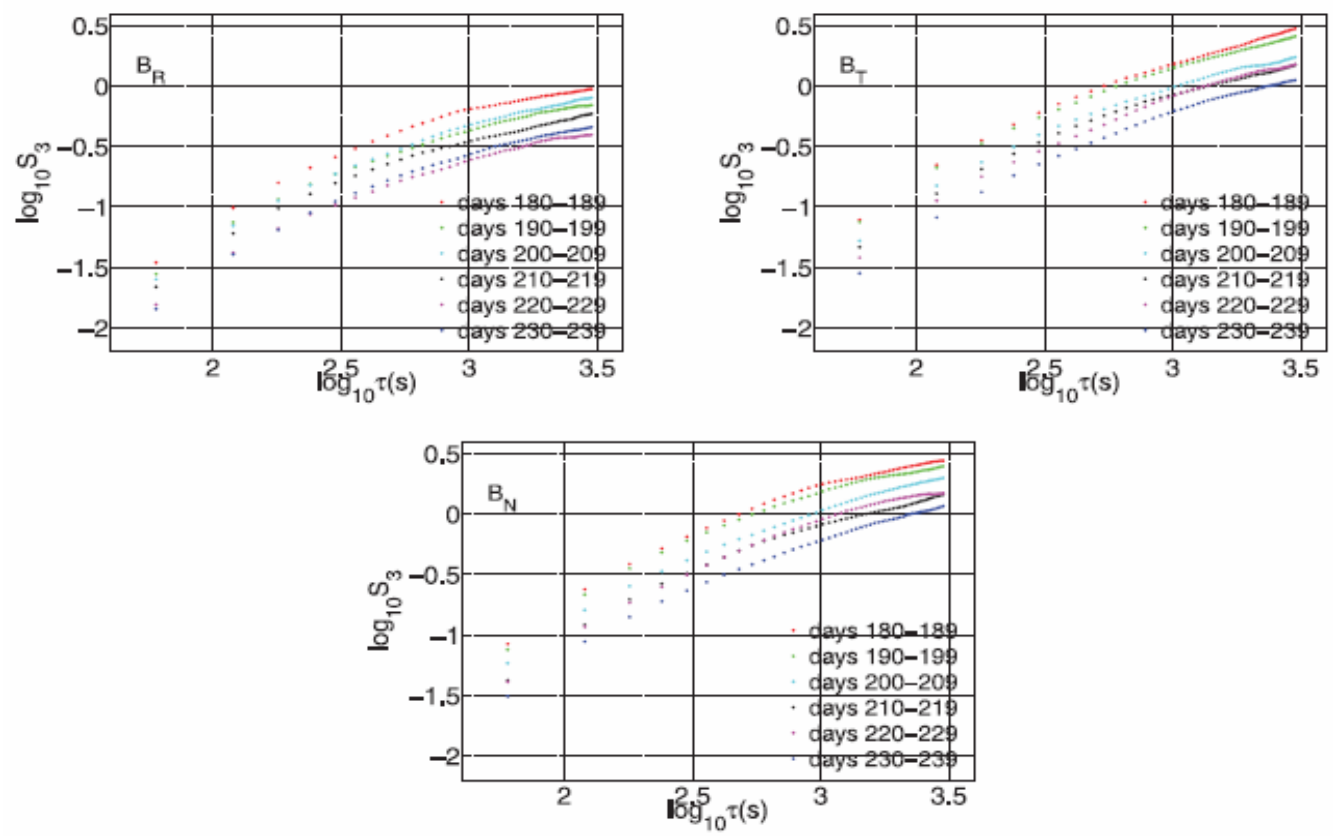

Significant curvature, hence not $S(p, \tau) \sim \tau^{ap}$. Evidence for a spectral break near $\log_{10}\tau = 3$
Systematic trends with increasing time, corresponding to greater heliocentric radial distance

CFSA centre for fusion, space and astrophysics

UKAEA Fusion Working in Europe

Extended self similarity in the solar wind

Logarithmic plots* of $S(p = 2, \tau)$ versus $S(p = 3, \tau)$

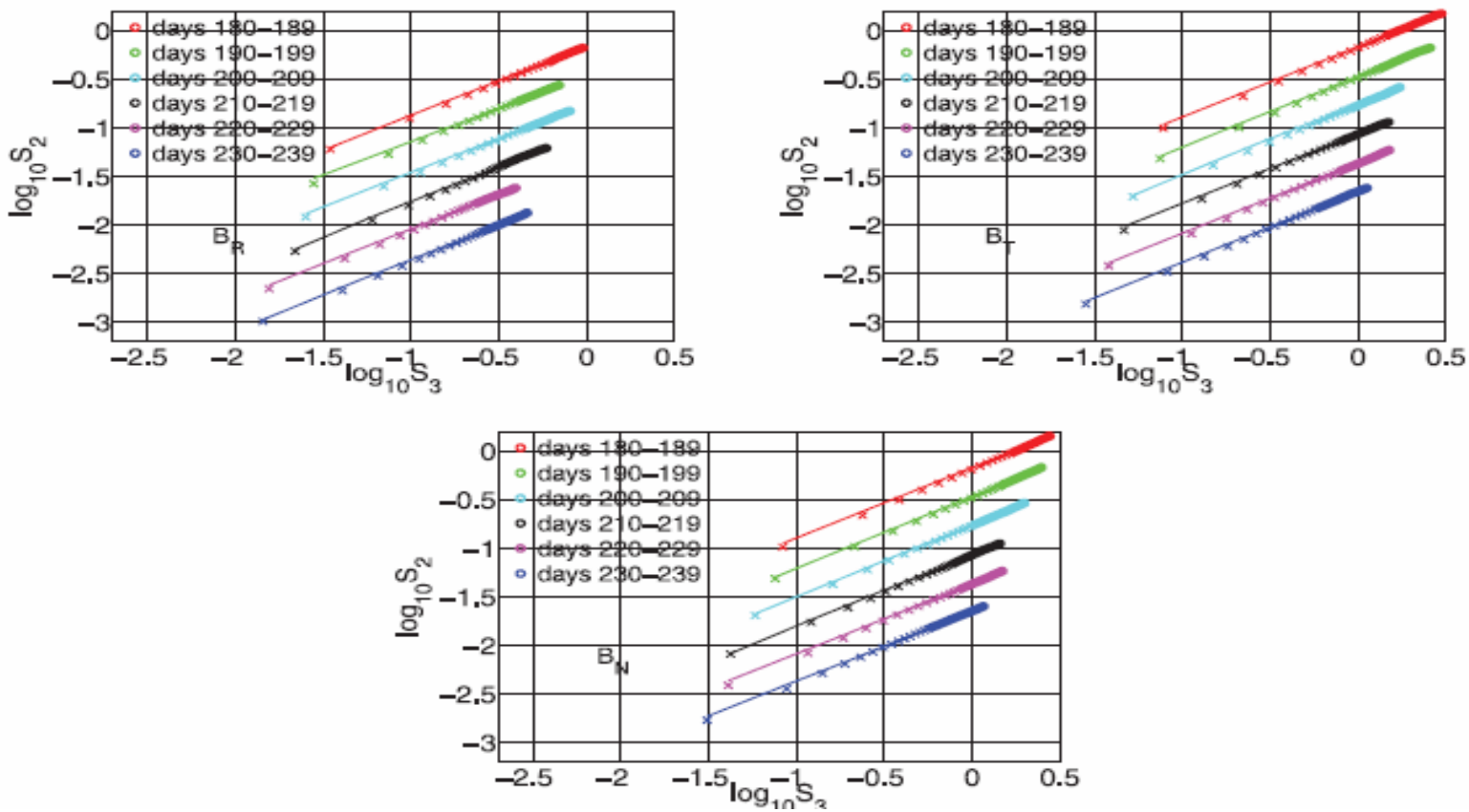

Evidence for $S(p = 3, \tau) \sim [S(p = 2, \tau)]^{\zeta(p=3)/\zeta(p=2)}$, where $\zeta(2)/\zeta(3) = 0.75$

*Nicol *et al*, *Astrophys J* **679**, 862 (2008)

CFSA centre for fusion, space and astrophysics

UKAEA Fusion Working in Europe

Tomaso Aste's (non-plasma-based) criteria* for complex systems

Complex systems

- exhibit **emergence:** some properties present at system level are not present at lower level — e.g. a cell is alive but is made of inanimate elements
- are **open:** energy and information are constantly being imported and exported across system boundaries
- have a **history:** the history cannot be ignored, even a small change in circumstances can lead to large deviations in the future
- can **adapt:** in response to external or internal changes, the system can reorganize itself without breaking — self organising
- are not completely **predictable:** when a system is adaptive, unexpected behaviours can emerge — prediction becomes expectation
- are **multi-scale** and **hierarchical:** system size and structure scale are over several orders of magnitude and distinct properties and functions are associated with different scales; dynamics can propagate through scales — avalanches, cascade effects
- are **disordered:** there is no compact and concise way to encode the whole information contained in the system
- have **multiple** (meta) (stable) **states:** small perturbations lead to recovery, larger ones can lead to radical changes of properties; dynamics do not average simply

**http://wwwrsphysse.anu.edu.au/~ccs106/SUMMERSCHOOLS/SS22/Proceedings/Themes.shtml*

Ornithophysical information flow

In the most successful model, each bird keeps an eye on about seven others

Quelea

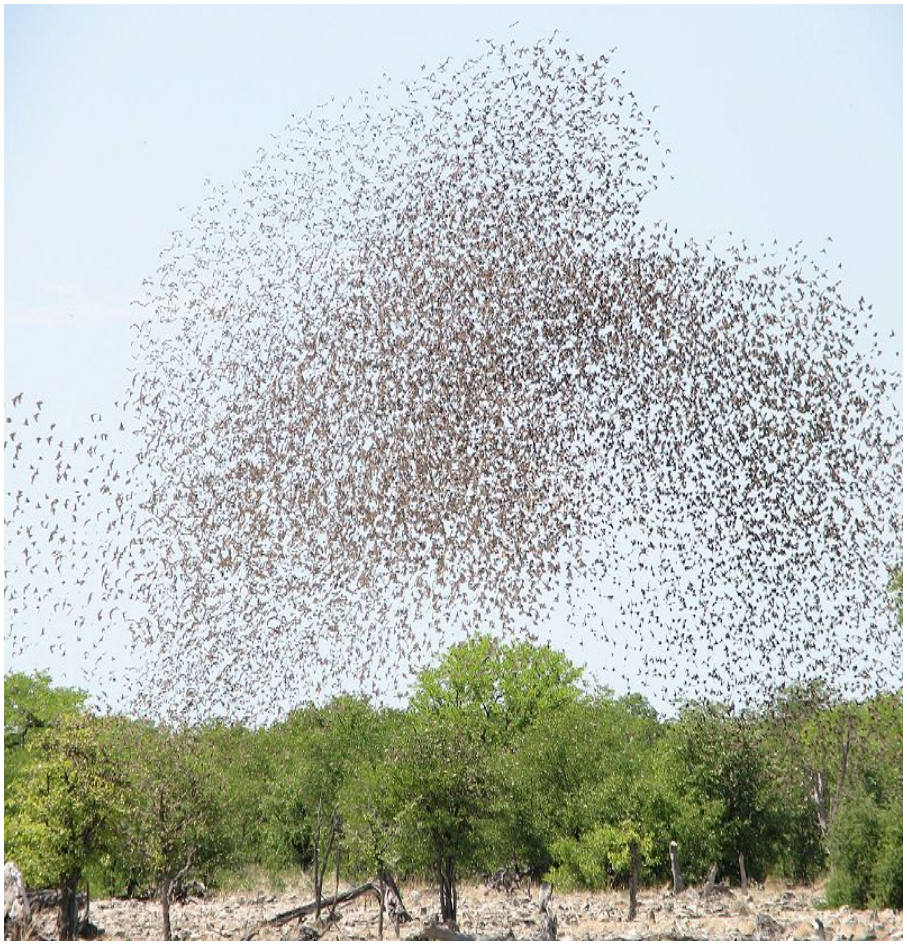

Starling

CFSA centre for fusion, space and astrophysics

UKAEA Fusion Working in Europe

And so to information…

- The typical very low density and high temperature of plasmas in magnetically confined fusion experiments implies a high degree of *disorder* at the lowest level of description, namely the self-consistent dynamics of charged particles and electromagnetic field.

- For this reason, *there is no compact and concise way to encode the whole information contained in the system:*
  - particle-in-cell codes which implement this lowest-level description are best adapted to phenomena occurring on the fastest timescales and shortest lengthscales
  - higher level descriptions are reduced models; to construct these, information has deliberately been dropped.

- So, for plasmas and for complex systems in general, what is the *information contained in the system*?

Quantifying physical linkage of two spatiotemporally separated, highly nonlinear, plasma signals: upstream solar wind and ionospheric

Solar wind from WIND satellite at sunward libration point

Terrestrial magnetometer data at high geomagnetic latitude

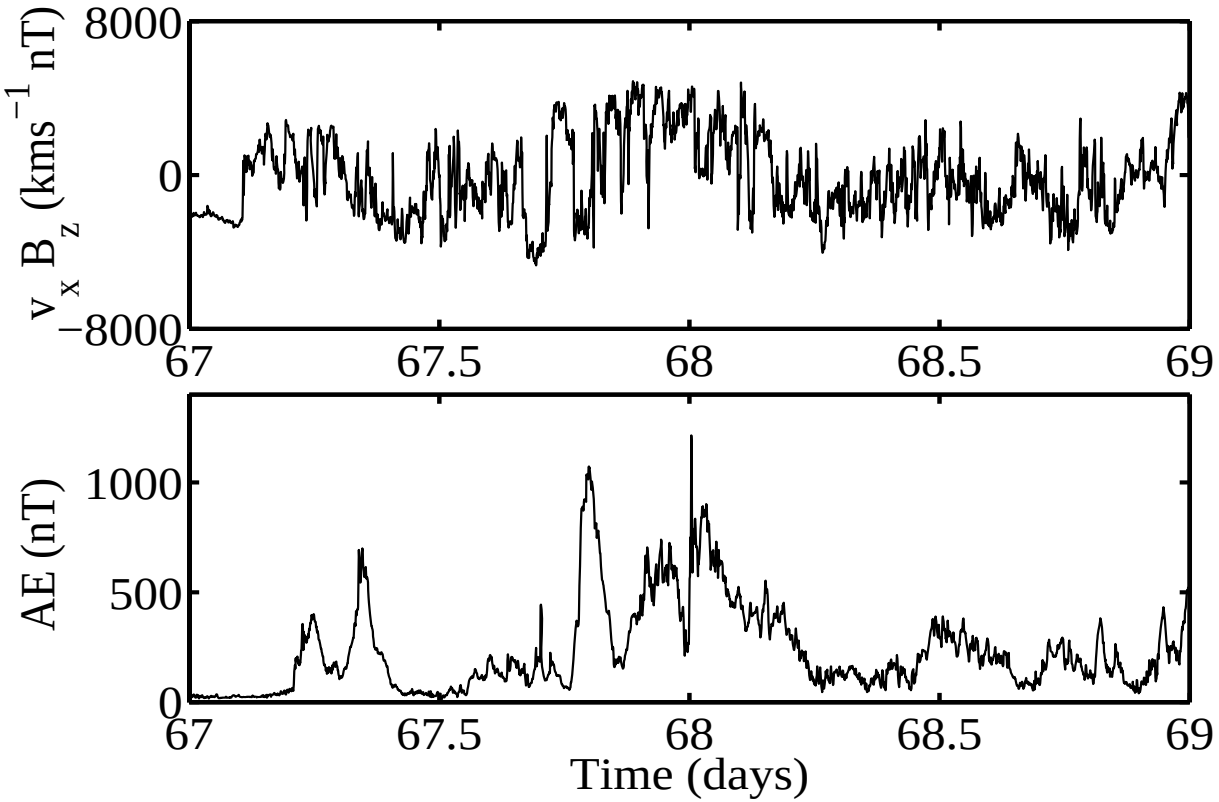

Solar wind drives magnetotail reconnection: energy release drives ionospheric currents affecting terrestrial magnetic field

CFSA centre for fusion, space and astrophysics

UKAEA Fusion Working in Europe

What is information?

Information resides in the number of yes/no (≡ binary 0/1) questions (≡ *bits*) to which we have the answer. E.g. for n = 3 questions there are:

2^3 = 8 possible combinations of yes/no answers, expressible as

8 three-digit (≡ three-bit) binary *symbols* 101, 110,…, etc.,

So in general *n bits* → an *alphabet* containing $M = 2^n$ *symbols*

Suppose we *sample* (ask n questions) the system on N occasions. The amount of *information* thereby obtained, H, is the number of questions to which we have answers:

$$H = N \times n = N \log_2 M$$

If all symbols occur with equal statistical probability $P = 1/M$, then

$$H = - N \log_2 P$$

Any digitally sampled measured signal is a time-ordered string of N n-bit symbols $X_1, X_2, .., X_i, \ldots, X_N$ drawn from an alphabet having $M = 2^n$ symbols.

Different symbols X_i recur N_i times, implying different empirical probabilities

$$P_i = N_i/N \neq 1/M$$

Information and signal measurement

Intuitively, the occurrence in the signal of a statistically rare symbol (small P_i, e.g. letter “x”) provides more information H than the occurrence of a frequent one (large P_i, e.g. letter “e”)

For the equal probability case, we also know $H = - N \log_2 P$ for N symbols, implying information per symbol = $H/N = - \log_2 P$

It appears logical to define the information gained from a single occurrence of X_i as $- \log_2 P_i$

In the signal of length N symbols, X_i occurs N_i times. So the total information provided by the occurrences of X_i is $H_i = - N_i \log_2 P_i$

The total information in the signal is then

$$H = \sum_i H_i = - \sum_i N_i \log_2 P_i = - \sum_i N P_i \log_2 P_i = - N \sum_i P_i \log_2 P_i$$

Hence the average information per symbol in a real signal is

$$h = H/N = - \sum_i P_i \log_2 P_i$$

This is the *Shannon Entropy* of the signal: “entropy” because of deep analogies with statistical mechanical entropy and, beyond, to thermodynamic entropy

Applying information theory to plasma data

Plasma systems typically yield highly nonlinear measurements – intermittent, bursty

Hence it may be suboptimal to try to identify correlation and causality via Fourier-derived techniques that rest upon the superposition of linear modes

Information-based analysis is intrinsically nonlinear, being based on sets of probabilities of arbitrary relative magnitude

The strategy is:

- Split each measured signal into a time-ordered string of symbols X_i
- Bin the data symbols to establish their probabilities P_i
- Calculate how information (meaning - $\sum_i P_i \log_2 P_i$ type quantities) is shared, flows, and decays, both
  - within a given signal
  - between two contemporaneous but separate signals

These techniques are widely in physics and engineering but remain “novel” in plasma physics

Defining linear cross covariance and mutual information

Both provide measures of correlation between two signals *A* and *B*.

Linear cross covariance

$$C(A,B) = \frac{E[(A-\overline{A})(B-\overline{B})]}{\sqrt{E[(A-\overline{A})^2]E[(B-\overline{B})^2]}}$$

where *E* [...] denotes the mathematical expectation value, and $\bar{A} = E[A]$.

Nonlinear mutual information

$$I(A,B) = \sum_{i,j}^{m} P(a_i,b_j)\log_2\left(\frac{P(a_i,b_j)}{P(a_i)P(b_j)}\right)$$

where signals *A* and *B* have been partitioned into exhaustive discrete alphabets $\{a_i\}$, $\{b_j\}$, with

- each symbol having empirical probability $P(a_i)$, $P(b_i)$,
- $P(a_i,b_j)$ is the joint probability of a_i and b_j

Quantifying clumpiness and flocking in complex systems, including plasmas

The Vicsek model* for flocking birds, fish,...

-Each flying bird (swimming fish...) takes account of the velocity orientation of its near neighbours, and does its best (subject to noise) to align with them

-Speed is constant, velocity orientation and position change

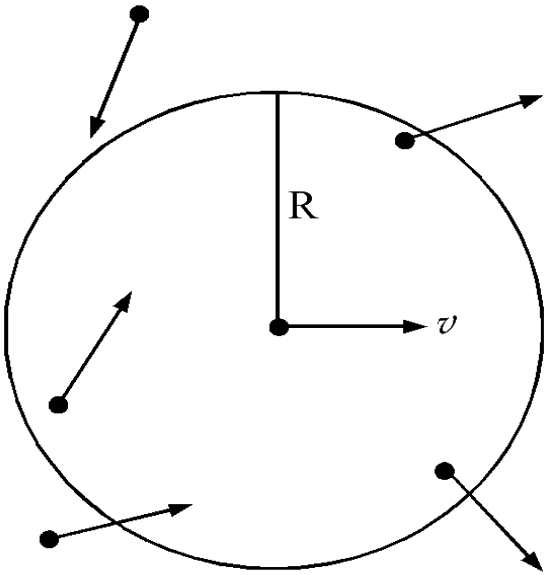

For each bird, at each successive time step:

-update position using current velocity

-identify the other birds within radius R, take their average velocity orientation, and add noise

$$x_{n+1} = x_n + \vec{v}\,\delta t$$

$$\theta_{n+1} = \langle \theta_n \rangle_R + \delta\theta_n$$

Noise range is $-\eta < \delta\theta < \eta$

*Vicsek, Czirok, Ben-Jacob, Cohen & Shochet, Phys. Rev. Lett. **75**, 1226 (1995)

CFSA centre for fusion, space and astrophysics

UKAEA Fusion Working in Europe

Critical phase transition at noise $\eta = \eta_c$ in the Vicsek model

At low noise level η,
a small number of flocks
form and move together
in roughly straight line

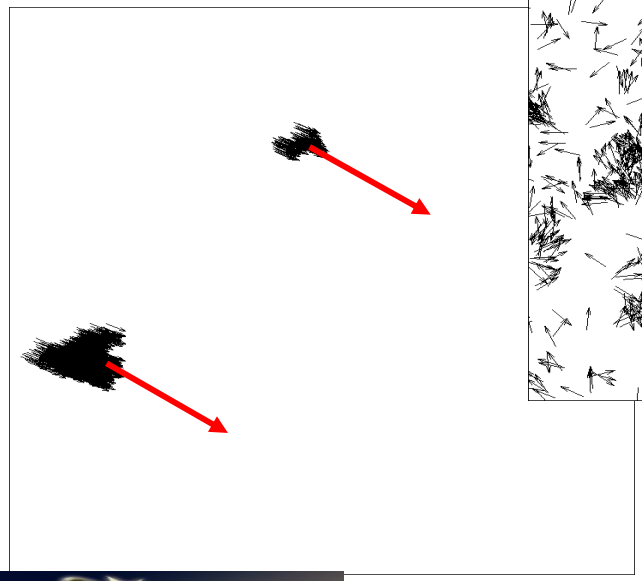

Structure on all
scales when $\eta \approx \eta_c$

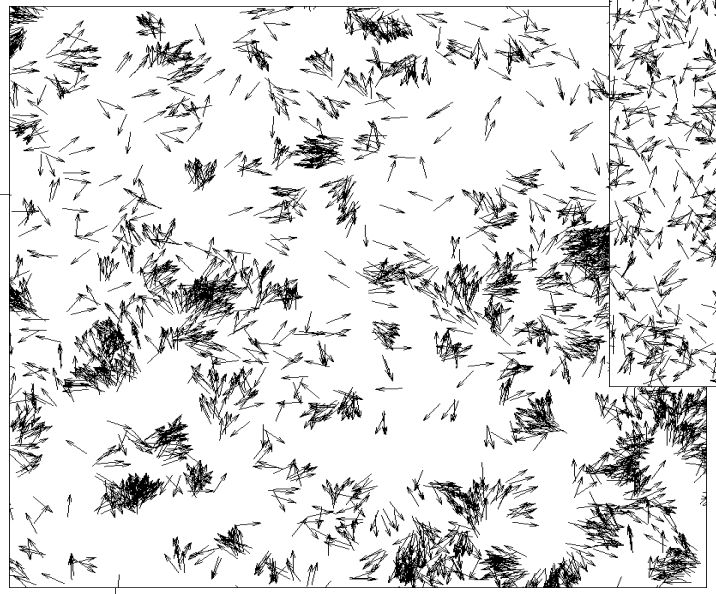

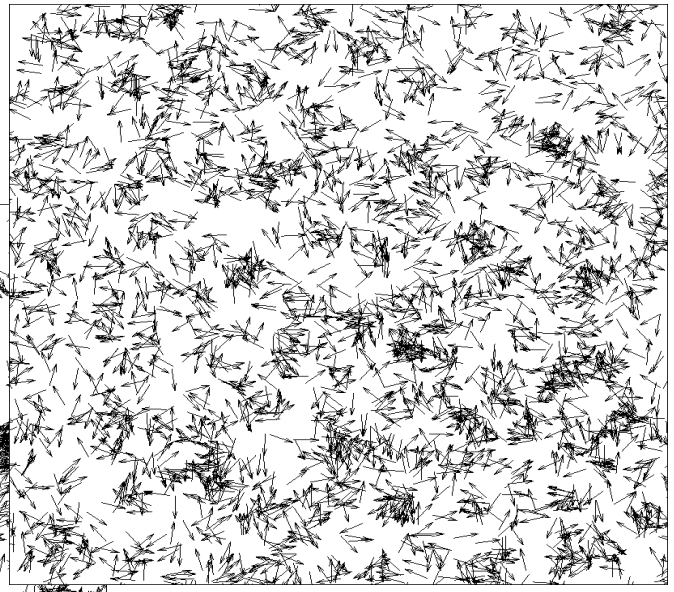

At high noise level η,
disordered Brownian motion

CFSA centre for fusion, space and astrophysics

UKAEA Fusion Working in Europe

Classical and information theory results for Vicsek

Plot measured mutual information (blue) and susceptibility (red) versus noise η

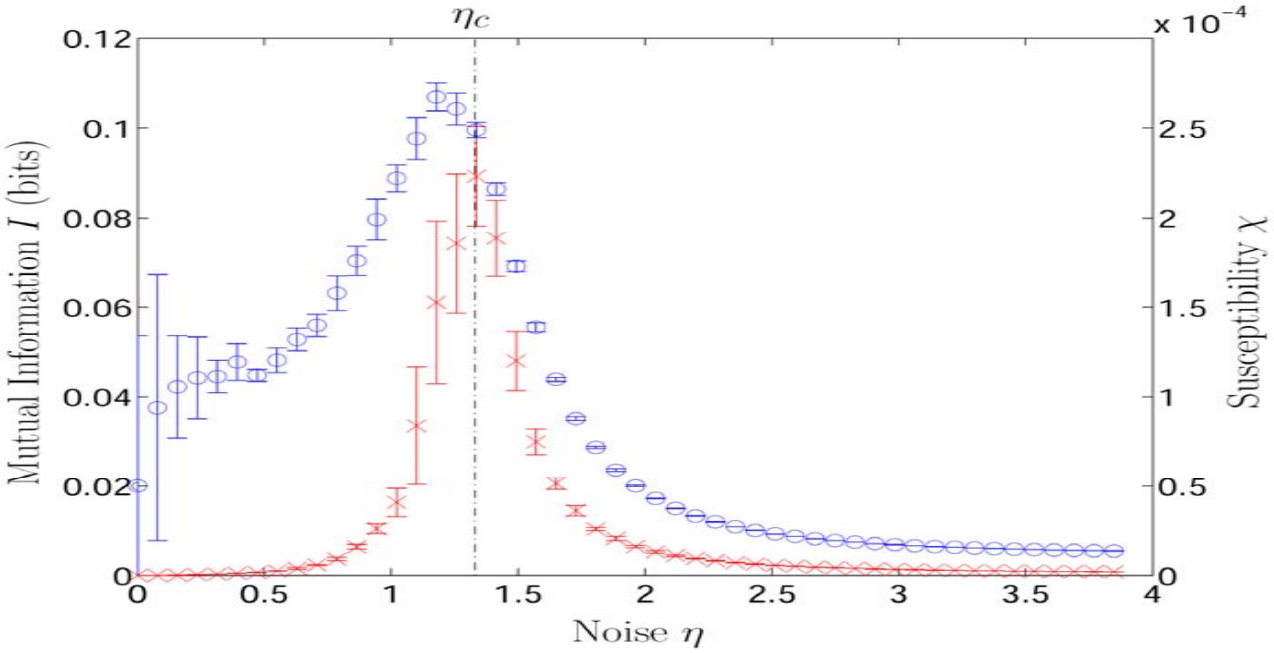

Error bars near the peak identifying the phase transition are

- at their smallest for mutual information

-at their largest for susceptibility

In this respect the intrinsically nonlinear measure is “better”

Wicks, Chapman & Dendy, Phys. Rev. E **75, 051125 (2007)*

CFSA centre for fusion, space and astrophysics

UKAEA Fusion Working in Europe

Quantifying physical linkage of two spatiotemporally separated, highly nonlinear, plasma signals: upstream solar wind and ionospheric

Solar wind from WIND satellite at sunward libration point

Terrestrial magnetometer data at high geomagnetic latitude

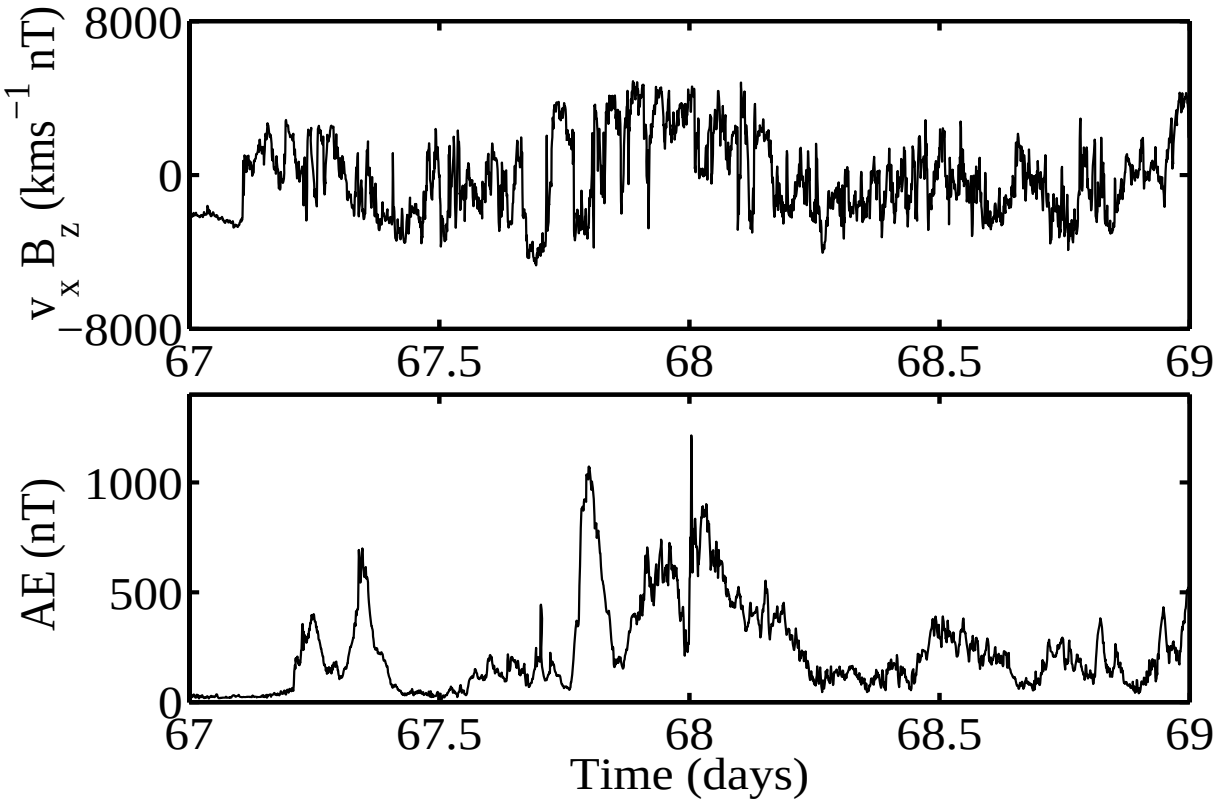

Solar wind drives magnetotail reconnection: energy release drives ionospheric currents affecting terrestrial magnetic field

CFSA centre for fusion, space and astrophysics

UKAEA Fusion Working in Europe

How much information do the solar wind and magnetometer data share in common?

March, Chapman and Dendy, *Geophysical Research Letters* **42**, L04101 (2005)

- Distinguish between hypotheses concerning solar wind propagation
  - Project ST data series in time according to different hypotheses for $\mathbf{v}_{sw}$ and $\mathbf{n}$:

    $\Delta t = (\mathbf{P}_w - \mathbf{P}_E) \,.\, \mathbf{n}/\mathbf{v}.\mathbf{n}$

- Time lag introduced by magnetospheric plasma processes
  - Additional $\Delta t'$ to accommodate this

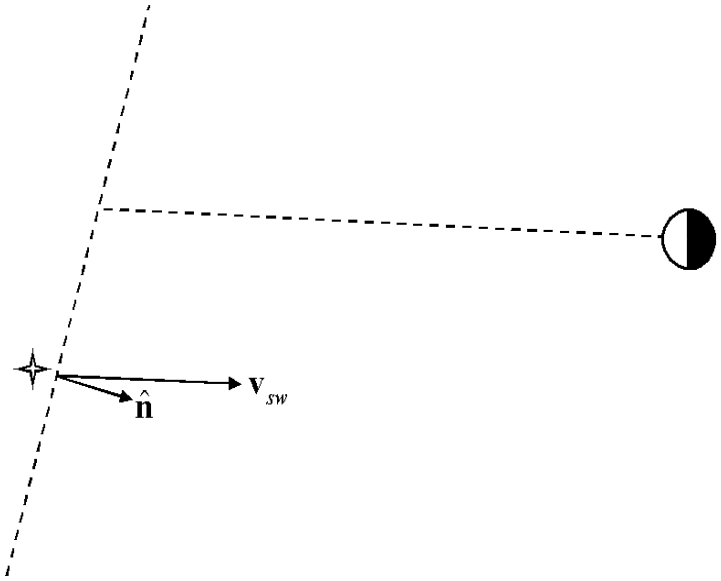

- Compute mutual information between SW(t) and AE ($t + \Delta t + \Delta t'$), and maximise

Mutual information between AE and SW

For four different SW propagation hypotheses, as a function of additional time lag $\Delta t'$

Physics output:

- Best hypothesis for propagation
- Shared information quantified
- Best time lag in magnetosphere

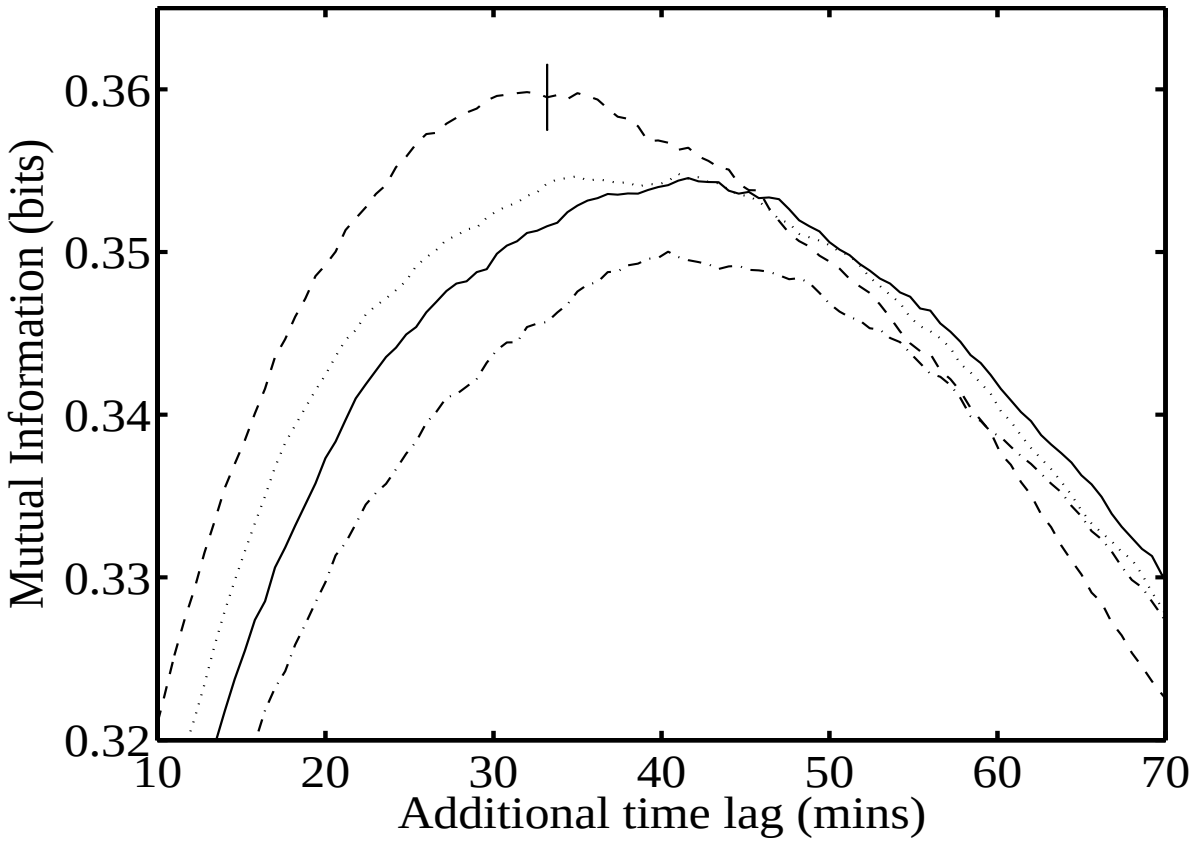

CFSA centre for fusion, space and astrophysics

UKAEA Fusion Working in Europe

Simultaneous two-spacecraft measurements in the solar wind

During 2005-2006 the WIND and ACE spacecraft were at the Sun-Earth libration point L_1 in the distant upstream solar wind – a near-ideal (remote boundaries, broad range of scales) turbulent plasma

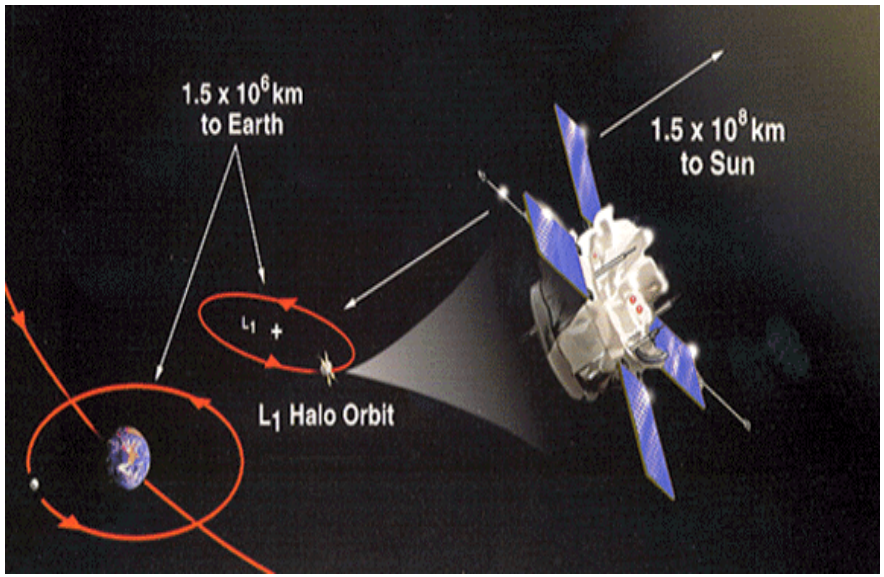

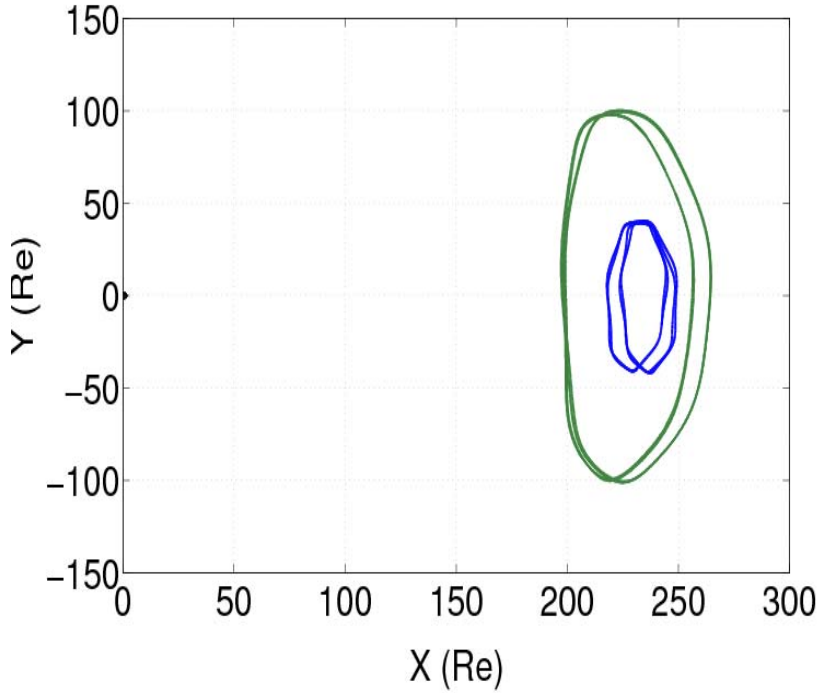

This enables measurements of spatial correlations in the measured, highly nonlinear, plasma and magnetic field properties of the solar wind, over a range 30 to 100 Earth radii (Re)

CFSA centre for fusion, space and astrophysics

UKAEA Fusion Working in Europe

Simultaneous solar wind measurements from WIND and ACE

Typical observations of B_x [nT] from WIND (blue) and ACE (red)

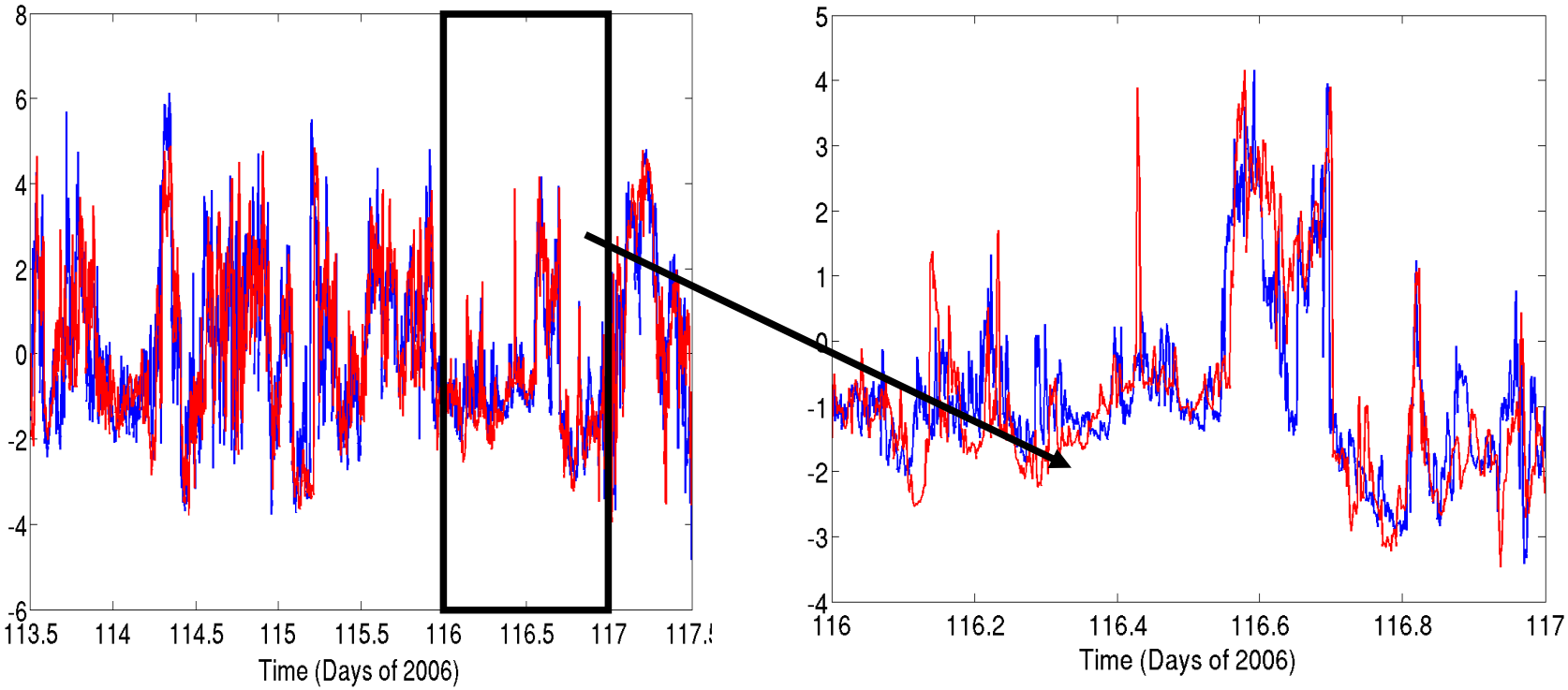

Four day trace

Embedded one-day trace

Strongly nonlinear signals exhibiting correlation across a range of timescales

CFSA centre for fusion, space and astrophysics

UKAEA Fusion Working in Europe

Mutual information measures the spatial decay of correlation

Density

Magnetic field strength

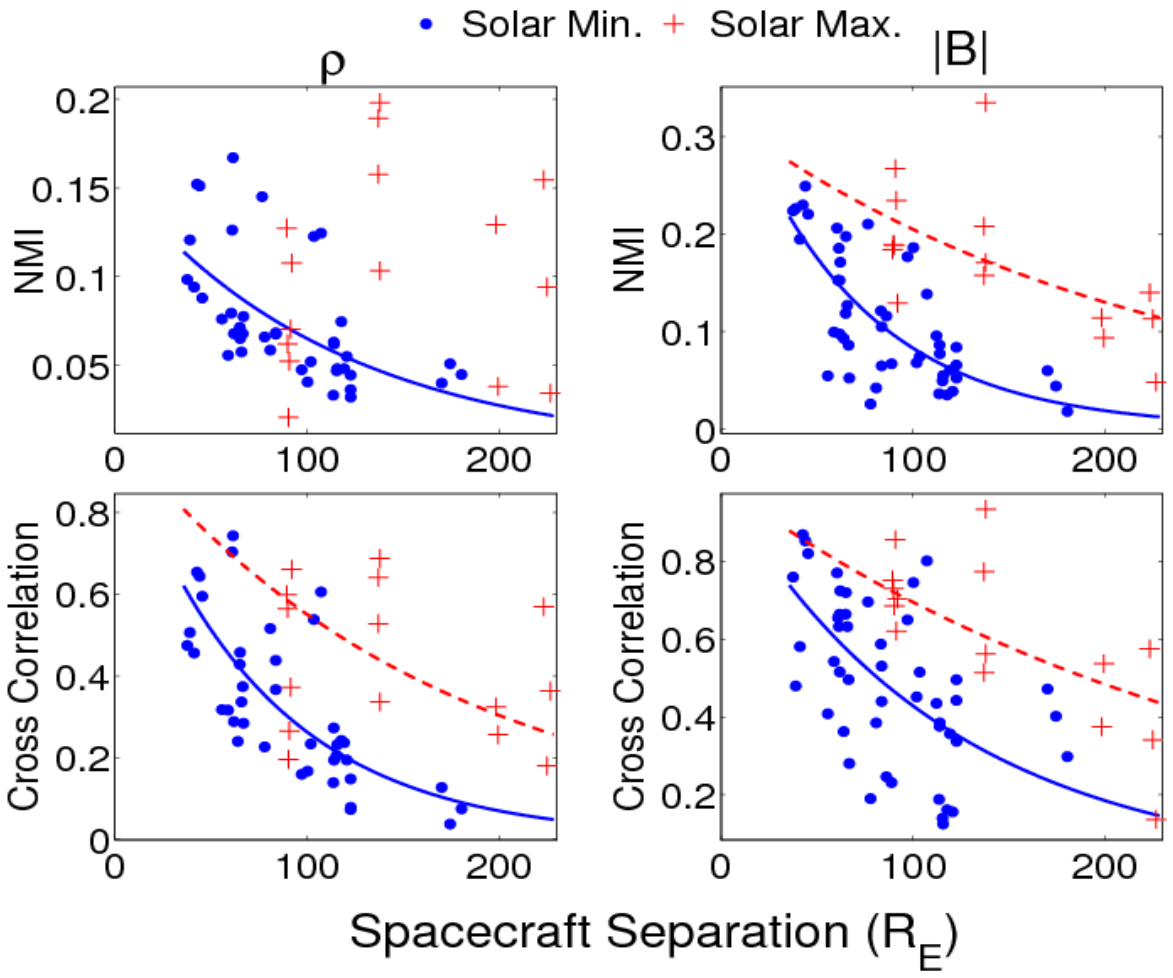

Mutual Information as described

Cross correlation

$$C(A,B) = \frac{E[(A-\overline{A})(B-\overline{B})]}{\sqrt{E[(A-\overline{A})^2]E[(B-\overline{B})^2]}}$$

Wicks *et al,* Astrophys J **690** 734 (2009)

These measurements enable us to distinguish between the different possible MHD characteristics (shear vs. compressional Alfvénic) of the turbulent structures

CFSA centre for fusion, space and astrophysics

UKAEA Fusion Working in Europe

Acknowledgments

Sandra Chapman, Joe Dewhurst, Bogdan Hnat, Thomas March, Noriyasu Ohno, Robert Wicks

CFSA centre for fusion, space and astrophysics

UKAEA Fusion Working in Europe

Aste's complex systems criteria as applied to plasmas (1)

- Plasmas in fusion and space exhibit *emergence*, meaning that *some properties present at system level are not present at lower level*.

- Overall energy confinement and release is a property that emerges only at *system level* from the interplay of *coupled* physical processes operating across a *hierarchy* of lower levels, reaching down to single particle dynamics.

- Each level of description (single fluid; two fluids – electrons and ions; kinetic ions and fluid electrons; gyrokinetic; and so on) within this hierarchy is determined by the characteristic lengthscale and timescale of whichever physical process dominates at that level. Plasmas are thus *multiscale*.

- The different levels of description and associated observed phenomenology *extend over several orders of magnitude, and distinct properties and functions are associated with different scales*.

- Plasmas self organise persistent coherent macroscopic structures that only arise on lengthscales at, or just below, *system level*. Examples include magnetic islands, zonal flows and magnetospheric boundary layers, which *are not present at lower level*.

Aste's complex systems criteria as applied to plasmas (2)

- Plasmas are invariably *open*, in the sense that *energy and information are constantly being imported and exported across system boundaries*.
- The quest for fusion power from magnetically confined plasmas involves injecting energy at the 10 MW level into a gram of material occupying a volume of tens of cubic metres. That such plasmas sustain, over seconds, the steepest steady-state temperature gradients known, while subject to energy fluxes of several MWm^{-2}, shows their ability to *adapt*: *in response to external or internal changes, the system can reorganize itself without breaking*.
- Plasmas are *not completely predictable*: *unexpected behaviours can emerge – prediction becomes expectation*. Performance in future experiments is extrapolated using empirical dimensionless scaling laws in the absence of first principles predictions of global phenomenology. Key behaviours, such as enhanced confinement operating regimes and ELMs, were not predicted.
- Transitions between confinement regimes typically have a *history*: *even a small change in circumstances can lead to large deviations in the future*, and reflect the existence of *multiple metastable states*. These transitions can occur spontaneously as plasma conditions evolve in time, or can be induced by careful sequencing of external drivers, notably auxiliary heating and fuelling. History is crucial and there is an element of irreversibility.

Information theory for plasmas is topical and exciting

Information theory may provide unifying principles for complex systems science and plasma physics.

Irrespective of their physical and mathematical embodiment, all complex systems have in common the creation, transmission, sharing and destruction of information.

- It is the ebb and flow, birth and death of information – a physical quantity – that underlies and enables the physical phenomenology.
- Quantifying the state and distribution of information within a complex system is thus crucial both to understanding its working, and to rigorously characterising its behaviour.
- We outline some pioneering studies of mutual information in the solar wind plasma upstream of Earth, using techniques tested on standard complex systems models for the collective dynamics (i.e., flocking) of birds.

Quantifying the phase change in the Vicsek model

Classical physics measures are
- "Order parameter" φ, in this case mean velocity

$$\phi = \frac{1}{N v_0} \left| \sum_{i=1}^{N} \underline{v}_i \right|$$

- "Susceptibility" χ, in this case velocity dispersion

$$\chi = \sigma^2(\phi) = \frac{1}{N} \left(\langle \phi^2 \rangle - \langle \phi \rangle^2 \right)$$

Information theory measure is derived from the probability distribution of the birds' positions and velocities $\{x_n, \theta_n\} \equiv A \equiv \{a_1, a_2, a_3, ...\}$: the "signal" comprising the "alphabet" (i.e., pre-assigned set of strings) a_i, each of which is found to occur with measured probability $p(a_i)$

From these probabilities we can construct the Shannon entropy

$$H(A) = -\sum_{i=1}^{n} P(a_i) \log_2 (P(a_i))$$

Given two such signals, we can measure their information theoretic correlation in terms of their normalised mutual information

$$NMI(A, B) = \frac{H(A) + H(B)}{H(A, B)} - 1$$

CFSA centre for fusion, space and astrophysics

UKAEA Fusion Working in Europe

Strategy for calculating mutual information for Vicsek system

1. Take a snapshot

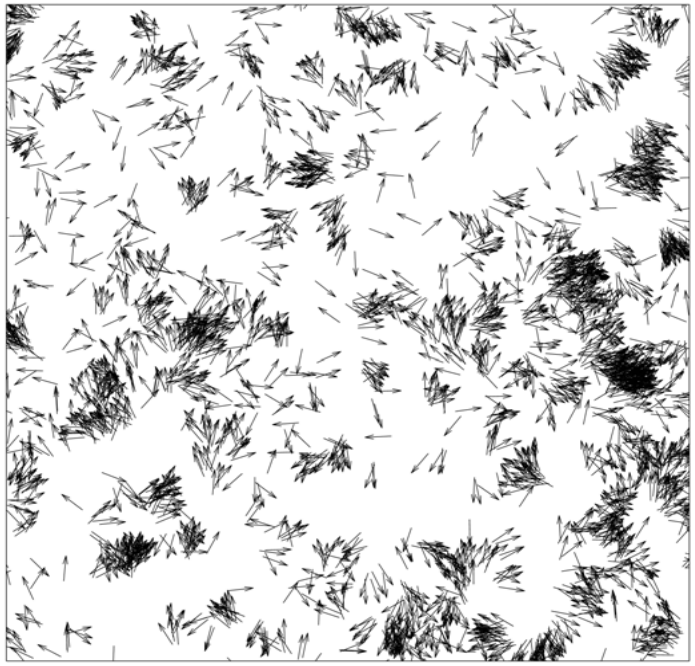

2. Discretise data – positions x and velocity orientations θ work best

3. Calculate entropies

CFSA centre for fusion, space and astrophysics

UKAEA Fusion Working in Europe

Measuring mutual information in the Vicsek system

Move from actual distributions to P(x), P(θ), and P(x, θ)

Raw data

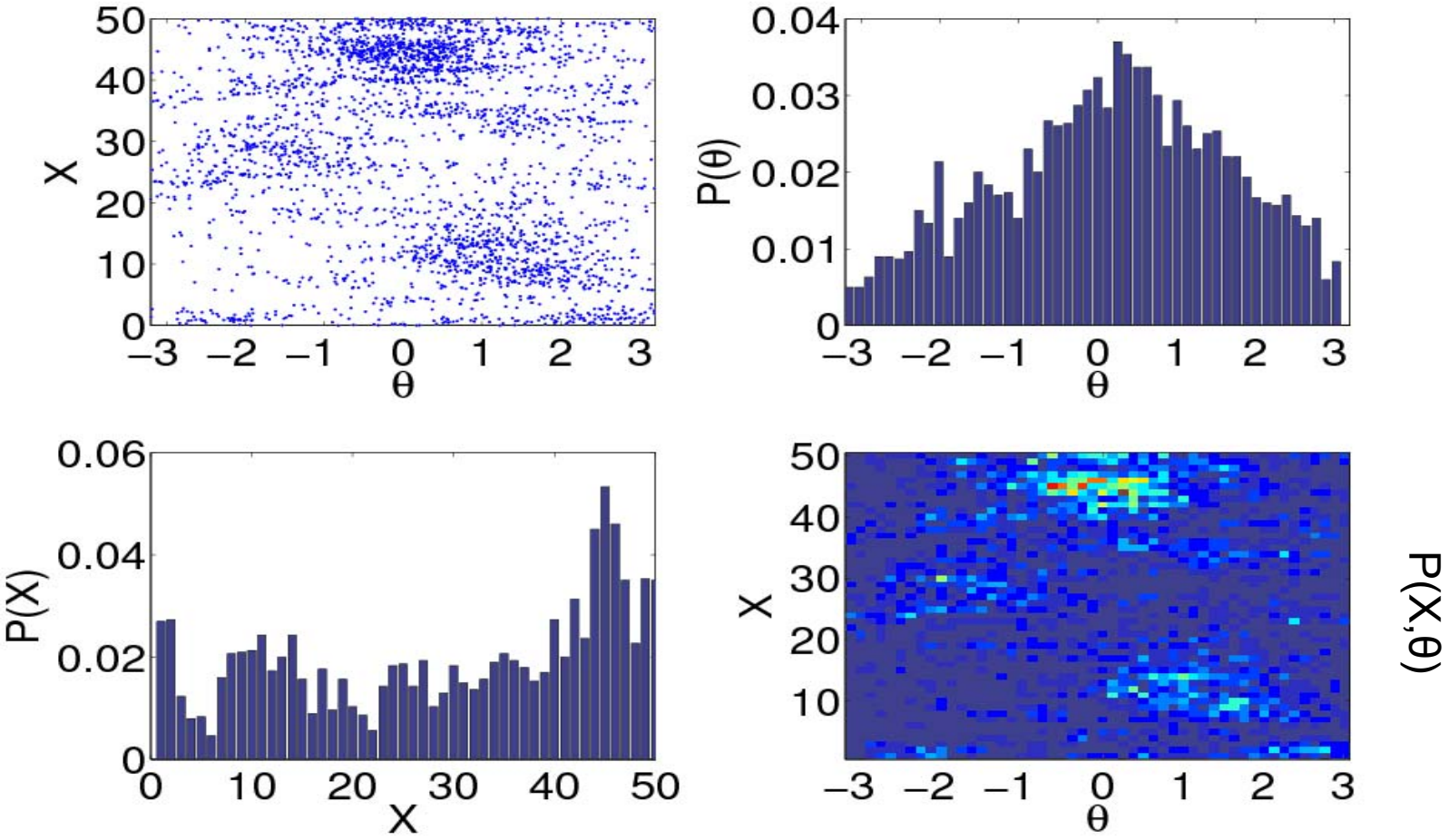

Spatial decay of correlation depends on solar activity in different ways

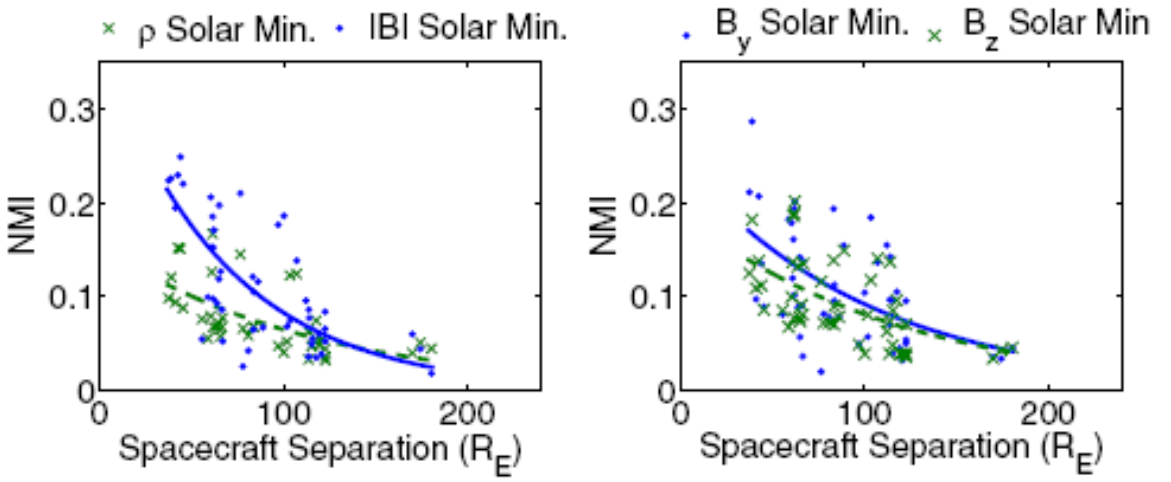

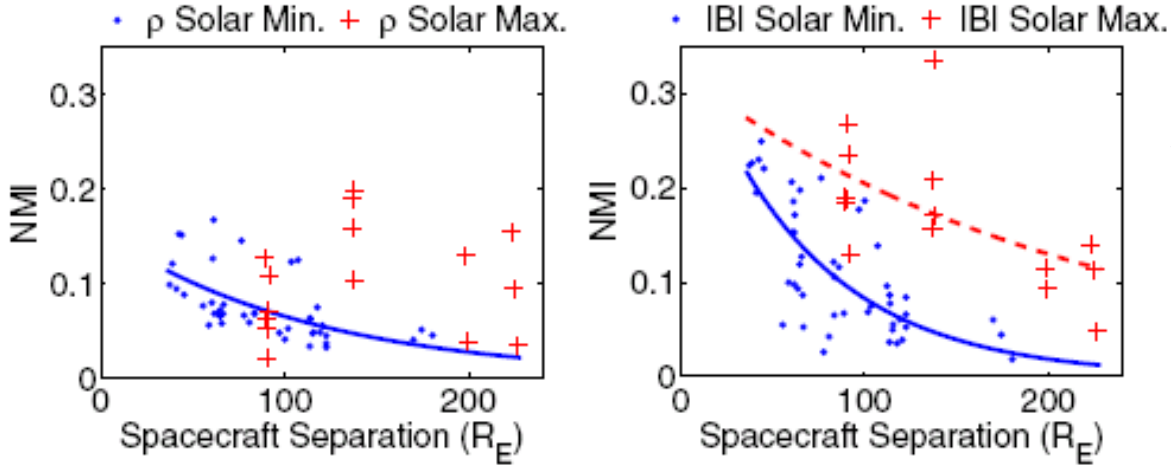

Correlation lengths λ(|B|) and λ(|ρ|) are twice as big at solar max than solar min, and vary together throughout the solar cycle

Correlation lengths $\lambda(B_x, B_y, B_z)$ do not change with solar cycle

These results may reflect different MHD characteristics (shear vs. compressional Alfvénic) of the nonlinear structures; or at larger scales, differences between structure synthesis in the solar corona and evolution in the solar wind

CFSA centre for fusion, space and astrophysics

UKAEA Fusion Working in Europe

Linear cross-correlation yields similar trends

Decay lengthscale of linear cross-correlation λ in units of Earth radii R_E

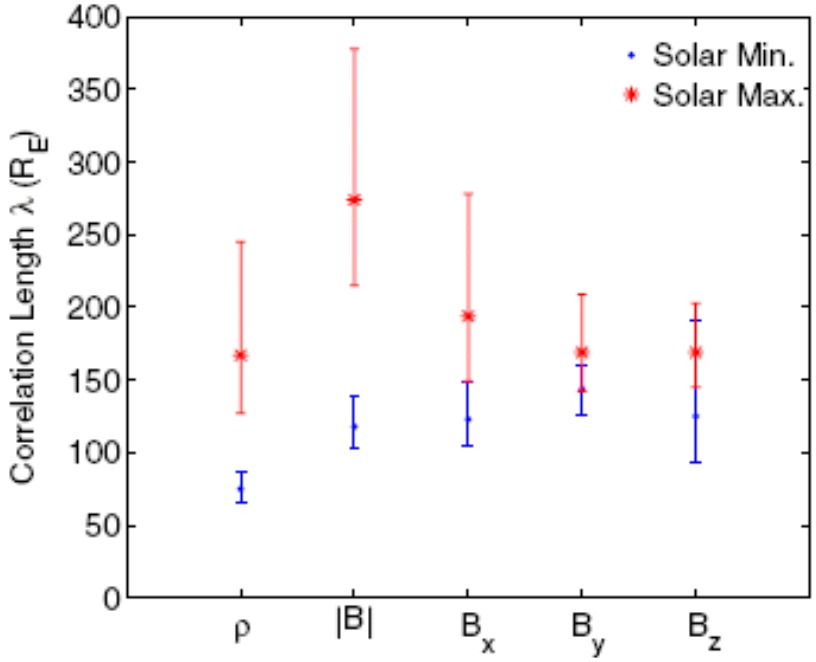

To compute cross-correlation, we need averages defined on a time window with duration τ:

- Short τ ~ 200 minutes enables us to resolve MHD turbulent fluctuations in the inertial range
- Long τ ~ 960 minutes averages over these, so that we focus on the 1/f range of propagating large scale fluctuations that may retain information about their coronal origin

We find solar cycle dependence of correlation measures is independent of window size

CFSA centre for fusion, space and astrophysics

UKAEA Fusion Working in Europe